


REVIEW ARTICLE

Physical sensors for skin-inspired electronics

Shuo Li | Yong Zhang | Yiliang Wang | Kailun Xia | Zhe Yin |
Huimin Wang | Mingchao Zhang | Xiaoping Liang | Haojie Lu |
Mengjia Zhu | Haomin Wang | Xinyi Shen | Yingying Zhang 

Key Laboratory of Organic
Optoelectronics and Molecular
Engineering of the Ministry of Education,
Department of Chemistry, Tsinghua
University, Beijing, China

Correspondence

Yingying Zhang, Key Laboratory of
Organic Optoelectronics and Molecular
Engineering of the Ministry of Education,
Department of Chemistry, Tsinghua
University, Beijing 100084, China.
Email: yingyingzhang@tsinghua.edu.cn

Funding information

National Key Basic Research and
Development Program, Grant/Award
Number: 2016YFA0200103; National
Natural Science Foundation of China,
Grant/Award Numbers: 21975141,
51672153; National Program for Support
of Top-notch Young Professionals, Grant/
Award Number: N/A

Abstract

Skin, the largest organ in the human body, is sensitive to external stimuli. In recent years, an increasing number of skin-inspired electronics, including wearable electronics, implantable electronics, and electronic skin, have been developed because of their broad applications in healthcare and robotics. Physical sensors are one of the key building blocks of skin-inspired electronics. Typical physical sensors include mechanical sensors, temperature sensors, humidity sensors, electrophysiological sensors, and so on. In this review, we systematically review the latest advances of skin-inspired mechanical sensors, temperature sensors, and humidity sensors. The working mechanisms, key materials, device structures, and performance of various physical sensors are summarized and discussed in detail. Their applications in health monitoring, human disease diagnosis and treatment, and intelligent robots are reviewed. In addition, several novel properties of skin-inspired physical sensors such as versatility, self-healability, and implantability are introduced. Finally, the existing challenges and future perspectives of physical sensors for practical applications are discussed and proposed.

KEYWORDS

electronics skin, flexible electronics, humidity sensors, mechanical sensors, temperature sensors, wearable sensors

1 | INTRODUCTION

Skin, the largest organ in the human body, plays important roles such as protection, metabolism, regulation, and sensation. Particularly, there are seven types of receptors in the skin for sensation, including pain receptors, two types of temperature receptors, and four types of mechanical receptors.¹ External stimuli are converted into electrical signals (action potentials) by the receptors, then the signals are transmitted to the brain through the nerves. Finally, under

the processing and instruction of the brain, the human body perceives and responds to the external stimuli.²⁻⁴ In recent years, inspired by the skin, novel electronics, such as wearable devices, electronic skin, and implantable electronic devices, have been widely studied, providing new opportunities for health monitoring, human disease diagnosis and treatment, and intelligent robots.^{3,5-9}

Development of various flexible physical sensors, including mechanical sensors, temperature sensors, humidity sensors, electrophysiological sensors, with high sensitivity, fast

This is an open access article under the terms of the Creative Commons Attribution License, which permits use, distribution and reproduction in any medium, provided the original work is properly cited.

© 2019 The Authors. *InfoMat* published by John Wiley & Sons Australia, Ltd on behalf of UESTC.

response, and high-resolution is the prerequisite for realizing the desired skin-mimic sensing functions.¹⁰ Mechanical sensors (pressure sensors and strain sensors), the most widely used physical sensors, can be applied to detect both vigorous human motions such as joint motions and subtle motions induced by blood pressure, pulse, breathing, sound, and so on.¹¹⁻¹⁹ Flexible temperature sensors can monitor body temperature in real time and thus assist with disease diagnosis and health monitoring.²⁰⁻²⁴ Humidity sensors can quantitatively detect skin hydration and environmental humidity.²⁵⁻²⁷ These kinds of physical sensors will be discussed in detail in Sections 2-4.

Furthermore, electrophysiological sensors can record important information about health by visualizing human body electrical signals into diagrams, such as the electrocardiogram (ECG), electromyogram (EMG), and electroencephalogram (EEG).²⁸⁻³⁶ Various flexible and conformable electrophysiological sensors have been developed for long-term monitoring electrophysiological signals. ECG is the best way to measure heart rhythms and has been widely used for diagnosing heart disease.³⁷⁻⁴⁰ EMG can record the electrical activity produced by skeletal muscles, which can be used to diagnose neuromuscular diseases and control prosthetic devices.⁴¹⁻⁴³ In addition, EEG can monitor the electrical activity of the brain and can be used to diagnose brain diseases (eg, epilepsy, sleep disorders).⁴⁴⁻⁴⁶

The signals accepted by the receptors in human skin will be transmitted to the central nervous system through neurons and synapses. Inspired by the sensory system, researchers integrated flexible electronics to acquire the signals and transmitted the acquired signals to motor nerves to actuate muscles.⁴⁷ Intrinsically stretchable organic conductors and semiconductors are highly desirable for applications in signals transmitting and processing.⁴⁸⁻⁵³ For example, Wang et al demonstrated a stretchable transistor array by using intrinsically stretchable conducting and semiconducting polymers. Based on this platform, they fabricated various intrinsically stretchable analog and digital circuits and integrated them with mechanical sensors to realize skin electronic systems.⁵²

With the development of skin-inspired electronics, higher demands are placed on flexible physical sensors. Firstly, it is necessary to increase the sensitivity, reduce the detection limit, and expand the monitoring range of the sensors. Secondly, the long-term monitoring of physical signals in daily life is required, which places flexible and stretchable demands for physical sensors. Moreover, as mechanical damages may happen to skin-inspired electronics due to wear or external forces, physical sensors also need to be self-healable. Given the widespread use of electronics, especially implantable electronics, physical sensors should have better biocompatibility and biodegradability.

In this study, we systematically review the latest advances of skin-inspired mechanical sensors, temperature sensors, and humidity sensors. The working mechanisms, materials, device structures, and performance of various physical sensors are summarized and discussed in detail. In addition, their applications for health monitoring, human disease diagnosis and treatment, and intelligent robots are described. Furthermore, the novel properties of skin-inspired physical sensors such as versatility, self-healability, and implantability are introduced. Finally, the existing challenges and future perspectives of physical sensors for practical applications are discussed and proposed.

2 | SKIN-INSPIRED MECHANICAL SENSORS

Mechanical sensors are sensitive to mechanical stimuli, which are commonly used to monitor body movements and physiological activities such as pulse, breath, heart-beat, and so on.⁵⁴ Mechanical sensors can be integrated into skin-inspired electronics, which can be applied in various fields. For example, in the robotic field, such sensors will allow robots to respond to external stimuli and accomplish complicated tasks.¹¹ In the medical field, mechanical sensitive electronics can not only help amputees regain sensory functions but also can be used to continuously monitor physiological health.^{4,55}

There are four kinds of mechanoreceptors in human skin, two of which are slow adapting receptors, which respond to static pressures.^{56,57} The rests belong to fast adapting receptors, which respond to dynamic forces.^{57,58} These receptors can convert external mechanical stimuli into electrical signals, the so-called action potentials, which are then transmitted to the brain through nerves. Based on this way, the skin can detect pressures greater than 2000 Pa with a time delay of 20-40 ms and a spatial resolution of 1 mm.^{2,59,60} With these four mechanoreceptors, human skin has a variety of mechanical sensing functions, including normal/shear force sensing, vibration detection, and strain monitoring. In 2000, Lee et al outlined ideal parameters for mechanical sensing skin-inspired electronics that the mechanical sensors need to be able to sense pressures greater than 1 g with a temporal resolution less than 10 ms and a spatial resolution less than 2 mm.⁶¹ According to the working mechanisms, mechanical sensors can be divided into several types, such as resistive type,¹⁶ capacitive type,¹⁷ piezoelectric type,¹⁸ triboelectric type,¹⁹ and other types (eg, optics type,⁶² wireless type⁶³). The details of skin-inspired mechanical sensors with various working mechanisms will be discussed in the following.

2.1 | Resistive-type mechanical sensors

Resistive-type mechanical sensors are the earliest available commercial mechanical sensors. The working mechanism of resistive-type mechanical sensors is on the change in the resistance of conductive materials during deformation, which can be easily measured by electrical measurement systems.^{64,65} The resistance (R) can be calculated by $R = \rho l/A$, where ρ is the material resistivity, l is the length of the conductor, and A is the sectional area. The change in resistance of some materials is mainly ascribed to the intrinsic resistivity change upon deformation, while that of other materials relies on the change of geometrical parameters (l and A). Therefore, the mechanism of the resistive-type mechanical sensors can be summarized as follows: (a) changes in intrinsic resistance; (b) changes in contact resistance (R_c).

The changes in the intrinsic resistance mainly originate from the change of the electronic band structure during deformation, which can be found in many materials such as semiconductors (Si,⁶⁶ Ge⁶⁷), carbon nanotubes (CNTs),⁶⁸ graphene,⁶⁹ and metal-organic framework (MOF).⁷⁰ Based on the hole transfer and conduction mass shift due to stress, the change in resistance of semiconductor has been widely used in mechanical sensors.^{66,67} The structure of the materials can significantly affect their sensing performance. He et al reported that the sensitivity of Si nanowires (NWs) is 37 times higher than that of bulk Si.⁷¹ Furthermore, unlike bulk Ge, Ge NWs show an anomalous negative resistance response (Figure 1A,B).⁷²

In addition, the band structures of the carbon nanomaterials (CNT, graphene) change along with

deformation. When deformed by an atomic force microscope tip, the conductance of a single-wall CNT sample reduced by two orders of magnitude, which provided the sensing ability for a single CNT (Figure 1C,D).⁶⁸ Bae et al fabricated a transparent graphene mechanical sensor, the resistance of which increased due to the change in the C—C bond length under tensile strain.⁶⁹

MOF is a kind of nanoporous materials formed by self-assembly of organic ligands and metal cations or clusters. Under mechanical stimuli, the electronic band structure and the intrinsic resistivity of MOFs can be changed due to the changing of the pore size (Figure 1E-G). Based on this, Pan et al reported the first MOF nanofilm-based mechanical sensor, which met the ultrasensitive and anti-jamming criteria for health monitoring and infrastructure failure diagnosis.⁷⁰

The changes in the contact resistance may originate from changes in the density of the conductive material, the contact area, and the conductive path induced by deformation. The mechanism of the contact resistance-based resistive-type mechanical sensors is shown in Figure 2A. Under the mechanical stimuli, the R_c changes more significantly than the intrinsic resistance and thus dominates the sensitivity. Most contact resistive-type mechanical sensors have a negative resistive effect, which means that the resistance decreases as the pressure increases.⁷⁵ For example, Pan et al reported an ultrasensitive resistive-type pressure sensor based on an elastic hollow-sphere polypyrrole (PPy) film. As shown in Figure 2B, the contact area between the conductive materials increases along with the pressure, leading to a decreased resistivity.⁷³

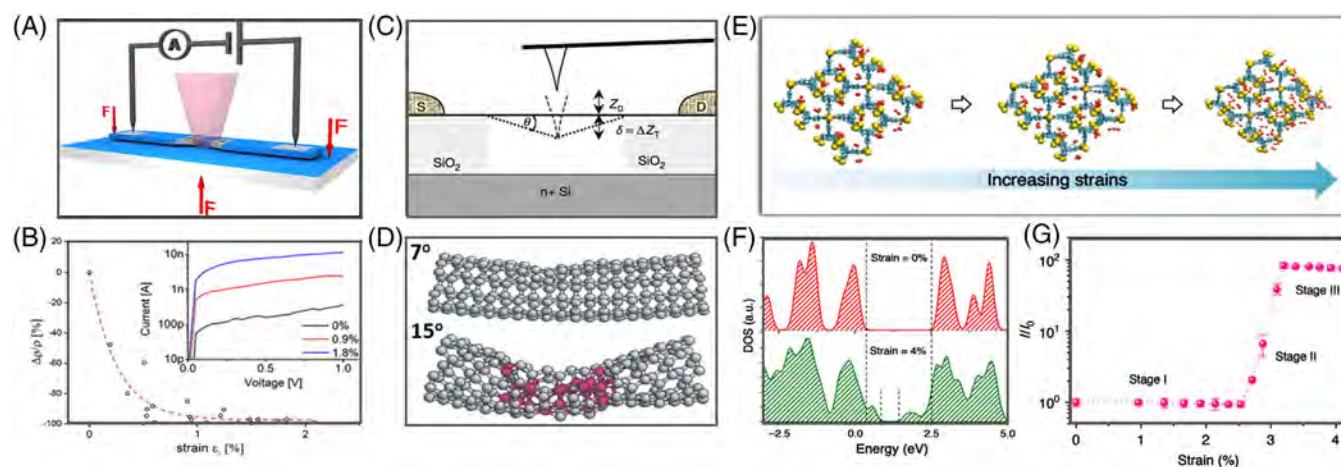


FIGURE 1 Resistive-type mechanical sensors based on intrinsic resistance. A, Device for measuring the intrinsic conductance of Ge nanowires. B, Resistivity of Ge change as a function of strain.⁷² Copyright 2012, American Chemical Society. C, Device for measuring the intrinsic conductance of CNT. D, Simulated atomic configurations of the nanotube pushed to 7° and 15°.⁶⁸ Copyright 2000, Springer Nature. E, Evolution of I₂@CuTCA MOF crystal structure. F, Local density of states of I₂@CuTCA MOF under strain. G, Evolution of the MOF device current as a function of strains.⁷⁰ Copyright 2018, Springer Nature. CNT, carbon nanotube; MOF, metal-organic framework

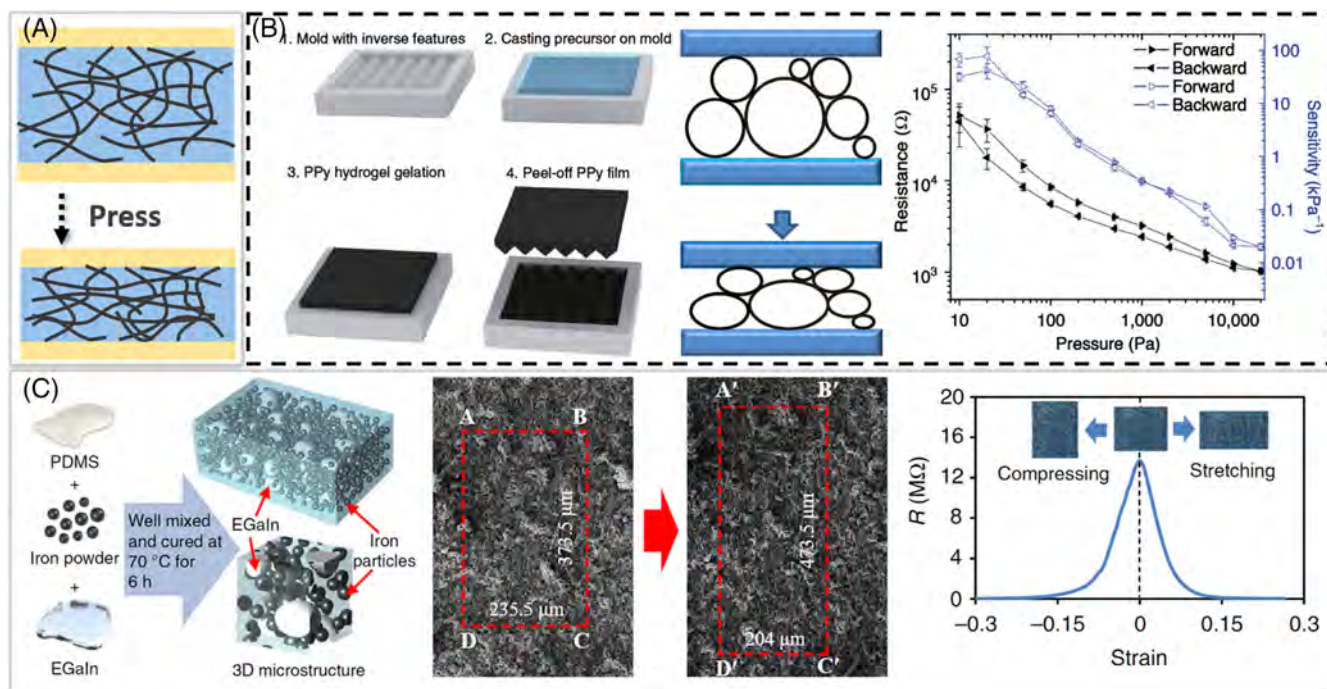


FIGURE 2 Resistive-type mechanical sensors based on contact resistance. A, Schematic diagram of contact resistance based resistive-type mechanical sensors. B, Conventional resistive-type pressure sensor based on hollow-sphere PPy.⁷³ Copyright 2014, Springer Nature. C, Unconventional positive piezoconductive mechanical sensor based on liquid metal-filled elastomer.⁷⁴ Copyright 2019, Springer Nature. PPy, polypyrrole

Contact resistive-type mechanical sensors with unconventional resistance changes draw much more attention. Yun et al reported a liquid metal-filled elastomer for mechanical sensors (Figure 2C).⁷⁴ The resistance of this sensor is maximum at its original state and decreases dramatically once deformed. As the Poisson ratio is 0.5, the mechanical sensor will be compressed in a certain direction upon any deformation, which will provide more conductive paths and induce decreasing of the resistivity.

The performance of resistive-type mechanical sensors is closely related to their components and device structures. Components used in the mechanical sensors can be divided into active materials and supporting materials. Metal-based materials (eg, liquid metals,⁷⁴ metal particles,⁷⁶ and NWs⁷⁷), carbon-based materials (eg, carbon black [CB],⁷⁸ CNT,^{79,80} and graphene^{13,15}), conductive polymers (eg, PPy,^{73,81} poly(3,4-ethylene dioxithiophene):poly(styrene sulfonate) [PEDOT:PSS],⁸² and hydrogel⁸³), and other materials (eg, MOF,⁷⁰ MXene^{84–86}) have been used as the active materials.

Most of mechanical sensors based on metals exhibit excellent electrical conductivity, good mechanical properties, and long-term stability. For example, Fan et al developed a transparent Ag NW network electrode with ultrahigh stability. The resistance of the electrode increased by less than 1% after 3000 bending cycles (Figure 3A).⁷⁷ As another good alternative, carbon materials have been

extensively employed to fabricate the mechanical sensors.⁹³ CB and graphite both present the possibility of industrial production and large-scale application due to their abundant source, low-cost, and facile preparation.⁷⁸ As novel carbon nanomaterials, graphene and CNT have been extensively studied in recent years. They have excellent electrical properties, superior stability, and can be easily functionalized, which enables the construction of the versatile mechanical sensors. For example, Xia et al reported fingerprint-like patterned 3D graphene films directly grown by chemical vapor deposition (Figure 3B), which can be used for pressure sensors with ultrasensitive (100 kPa^{-1}) and fast response ($<30 \text{ ms}$).¹⁵ In addition, biomass-derived carbon materials (such as from silk, cotton, mushrooms, and corncobs), which have advantages of renewable sources, mass production, and environmentally friendly, have also been used in skin-inspired mechanical sensors.^{94–97}

In addition, conductive polymers with better processability and stretchability, have been widely used as active materials for mechanical sensors. For example, He et al reported a highly stretchable conductive network by interpenetrating PPy into polyurethane, which can be used to prepare stretchable electronics with arbitrary shape and size.⁸¹ PEDOT:PSS is another common conductive polymer. You et al employed polyurethane microspheres coated with PEDOT:PSS to fabricate a high-resolution

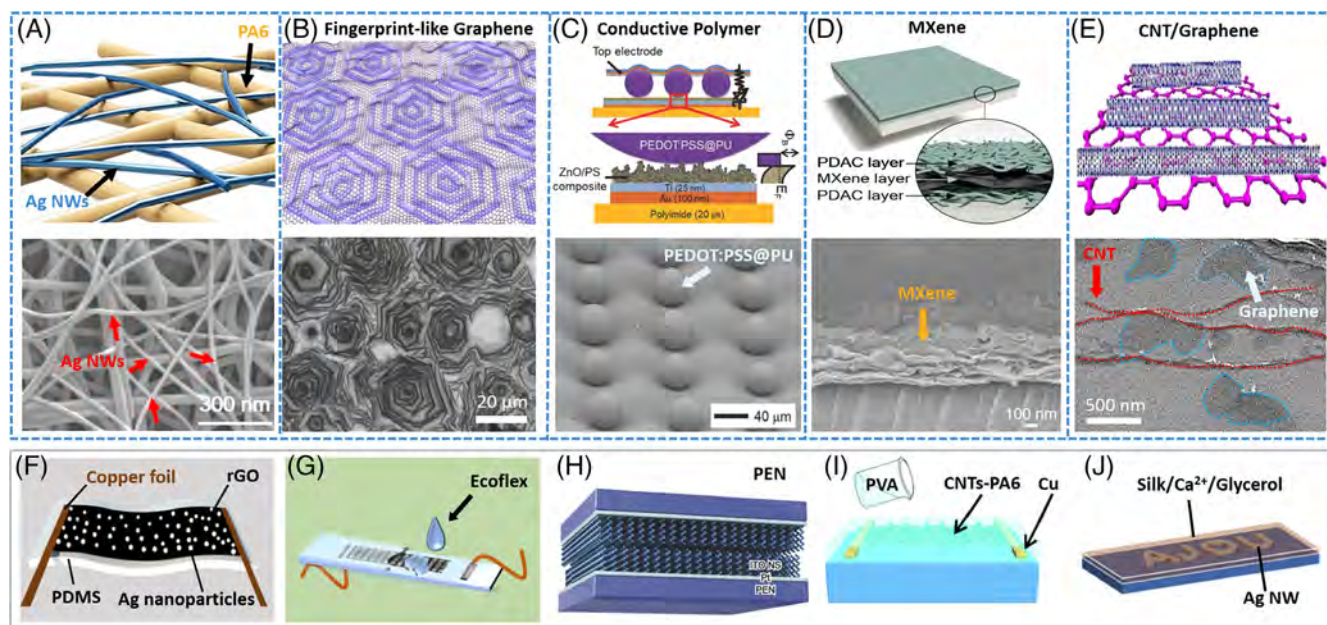


FIGURE 3 Various active materials and supporting materials used in resistive-type mechanical sensors. A, Metal materials (AgNWs).⁷⁷ Copyright 2018, American Chemical Society. B, Carbon materials (graphene).¹⁵ Copyright 2018, Tsinghua University Press and Springer-Verlag GmbH Germany. C, Conductive polymers (PEDOT:PSS).⁸² Copyright 2018, Wiley-VCH. D, Other materials (MXene).⁸⁶ Copyright 2018, AAAS. E, Hybrid materials (CNT/graphene).⁸⁷ Copyright 2017, Wiley-VCH. F, Silicone (PDMS).⁸⁸ Copyright 2018, American Chemical Society. G, Silicone (Ecoflex).⁸⁹ Copyright 2017, Wiley-VCH. H, Polymer (PEN).⁹⁰ Copyright 2018, Wiley-VCH. I, Hydrogel (PVA).⁹¹ Copyright 2017, Royal Society of Chemistry. J, Biomaterial (fibroin).⁹² Copyright 2018, American Chemical Society. CNT, carbon nanotube; NW, nanowires; PDMS, polydimethylsiloxane; PEDOT:PSS, poly(3,4-ethylene dioxythiophene):poly(styrene sulfonate); PEN, polyethylene naphthalate; PVA, polyvinyl alcohol

flexible mechanical sensor for Braille recognition (Figure 3C).⁸² MXene, emerging recently, is a 2D-layered nanomaterial with high conductivity and large specific surface area. MXene has also been used for flexible mechanical sensors. For example, a conductive, stretchable, and bendable MXene mechanical sensor using the layer-by-layer assembly process has been reported (Figure 3D).⁸⁶ In addition, two or more kinds of conductive fillers can be used synergistically to achieve better performance. For example, Jian et al prepared a CNT/graphene hybrid film and demonstrated its superior performance in a highly sensitive pressure sensor (Figure 3E).⁸⁷ Due to their synergistic effect, the pressure sensor showed a high sensitivity (19.8 kPa^{-1}) and ultralow detection limit (0.6 Pa).

Apart from active materials, the supporting materials also significantly influence the performance of mechanical sensors. There are several kinds of commonly used supporting materials in flexible mechanical sensors, such as polymers, silicone (eg, polydimethylsiloxane [PDMS], Ecoflex),^{88,89} polyacrylic ester (PEA),⁹⁸ and polyethylene naphthalate (PEN)⁹⁰, hydrogels (eg, polyvinyl alcohol (PVA),⁹¹ polyacrylamide⁹⁹), and biomaterials (eg, fibroin^{92,100}). Silicone is one of the most widely used supporting materials due to its good

flexibility, high stretchability, and satisfying biocompatibility. As a comparison, PDMS is more transparent, while Ecoflex has a higher stretchability. For example, Ag nanoparticles and graphene have been incorporated with PDMS for constructing of strain sensors with high sensitivity and wide measurement range. The PDMS provided good flexibility, high stretchability, and well durability to the sensor (Figure 3F).⁸⁸ Zhang et al encapsulated carbonized plain cotton fabric in Ecoflex and prepared a strain sensor with a large measurement range ($>140\%$) and a low detection limit (0.02%) (Figure 3G).⁸⁹ However, due to the viscoelasticity of the silicone matrix, mechanical sensors using silicone as a packaging material usually exhibit inevitable hysteresis.

In addition to silicone, there are other good choices for the supporting materials of mechanical sensors. Firstly, transparent, flexible, stretchable, and corrosion-resistant polymers (eg, PEA, PEN) have been used in mechanical sensors. For example, Chun et al fabricated interlocked indium tin oxide (ITO) nanosprings on PEN for a fast-response (submillisecond) pressure sensor (Figure 3H).⁹⁰ Also, hydrogels, showing good hydrophilicity, adjustable mechanical properties, and excellent biocompatibility, are widely used in biomedical fields. For example, Wang et al fabricated a CNTs-polyamide nanofiber-based conductive

composite for strain sensor.⁹¹ They chose PVA as the matrix due to its high hydrophilicity and high film-forming ability (Figure 3I). In addition, biomass materials, which possess excellent biocompatibility and controllable biodegradability can also be used as supporting materials in mechanical sensors. For example, Jo et al reported a protein-based electronic skin that combines Ag NWs and silk fibroin. The silk fibroin substrate provided a biocompatible and molecular permeable matrix, which allows the electronic skin to be capable of sensing strain, electrochemical signal, and electrophysiological signal (Figure 3J).⁹²

In addition to the selection of materials, the design of device structures also has a tremendous influence on the performance of mechanical sensors. For example, mechanical sensors with structures such as waves, ribbons, serpents, 3D spirals, and meshes, which endow the mechanical sensors with high stretchability, have been developed.¹⁰¹

In addition, conductive fabric-based mechanical sensors with unique hierarchical fiber networks have been developed.¹⁰² One method to prepare a conductive fabrics is coating conventional fabrics with conductive materials (eg, CB,¹⁰³ ZnO,¹⁰⁴ and graphene^{105,106}). Another method is carbonizing fabrics which are mainly comprised of

cotton,⁸⁹ silk,^{94,107} and so on. For example, Luo et al reported a resistive-type sensor based on a CB-coated fabric for blood pressure measurement (Figure 4A).¹⁰³ The sensitivity of the pressure sensor can be adjusted by tuning the loading ratio of CB. Wang et al developed a strategy for fabricating ultrastretchable strain sensors based on carbonized silk fabrics, which showed high sensitivity in a strain range up to 500% due to the unique woven structures (Figure 4B).⁹⁴ Fabric-based mechanical sensors with different woven structures perform different electro-mechanical responses. A strain sensor from carbonized silk georgette, which is composed of twisted yarns in both warp and weft directions, exhibited higher sensitivity than sensors based on other silk fabrics (plain wave, satin wave, twill wave).¹⁰⁷ Also, fabrics with interlocking structures can show a negative electrical resistance response, which means that the electrical resistance decreases along with loading of stretching (Figure 4C).¹⁰⁵ In addition, the interlocking microstructure can introduce high elasticity, stretchability, sufficient roughness, and more conductive pathway. Based on this, Yin et al fabricated a graphene/polyamide interlocking pressure sensor with high sensitivity (2.34 kPa^{-1}), wide sensing range (up to 80 kPa), and low detection limit ($<1.38 \text{ Pa}$).¹¹²

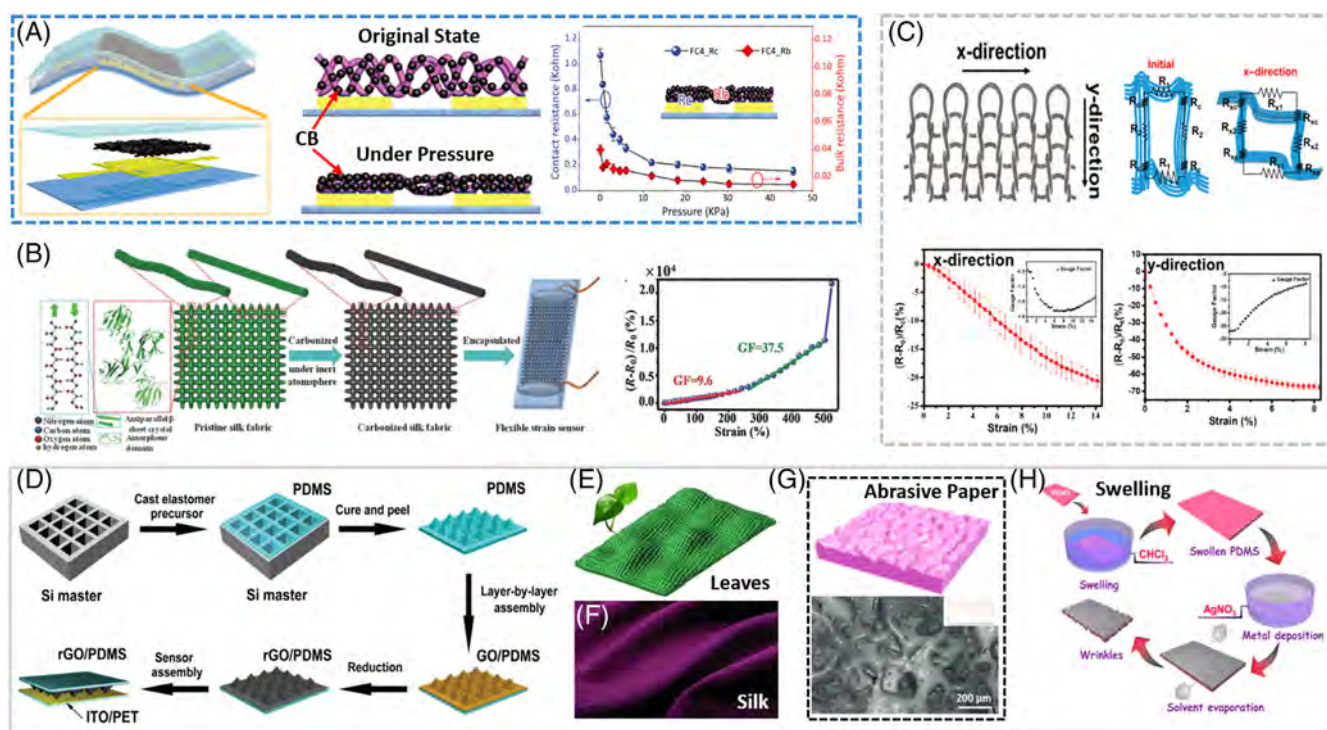


FIGURE 4 Structures of resistive-type mechanical sensors. A-C, Fabric-based mechanical sensors: A, coating fabric with CB,¹⁰³ Copyright 2016, Wiley-VCH. B, Carbonized silk fabric.⁹⁴ Copyright 2016, Wiley-VCH. C, Negative resistance response mechanical sensor with interlocking structures.¹⁰⁵ Copyright 2018, American Chemical Society. D-G, Microstructured surface by template transfer method: D, pyramid-structured Si molds.¹⁰⁸ Copyright 2014, Wiley-VCH. E, Leaves.¹⁵ Copyright 2018, Tsinghua University Press and Springer-Verlag GmbH Germany. F, Silk.¹⁰⁹ Copyright 2013, Wiley-VCH. G, Abrasive paper.¹¹⁰ Copyright 2018, American Chemical Society. H, Ag wrinkles by polymer swelling.¹¹¹ Copyright 2016, American Chemical Society. CB, carbon black

In addition to the macrostructures, the microstructures of the supporting materials and active materials also have a significant influence on the sensor's performance. Human fingertip skin, where there are many epidermal ridges to amplify external stimuli, has high sensitivity. Therefore, mimicking human fingertip skin with a rough surface is a potential way to obtain a highly sensitive mechanical sensor. To this end, transferring active materials to a template with a rough surface, such as microstructured Si molds,¹⁰⁸ leaves,¹⁵ silk,¹⁰⁹ abrasive paper,¹¹⁰ and so on, is usually implemented (Figure 4D–G).

However, the transfer process is generally complicated, costly, and time-consuming. Therefore, other facile methods for obtaining microstructures are highly demanded. The microstructured supporting materials can also be realized by exploiting the mechanical imbalance of heterostructures caused by external stimuli such as heat treatment and swelling.^{111,113} As schematically illustrated in Figure 5H, conductive Ag wrinkles can be deposited on PDMS by polymer swelling.¹¹¹

In conclusion, the performance of resistive-type mechanical sensors is closely related to their components

and device structures. The details of main features of skin-inspired resistive-type mechanical sensors based on different materials and structures are summarized in Table 1.

2.2 | Capacitive-type mechanical sensors

Capacitive-type mechanical sensors can convert mechanical stimuli into capacitance changes. The working mechanism and some typical capacitive-type mechanical sensors are shown in Figure 5A. The capacitance (C) of a capacitor can be calculated by $C = \epsilon_r A / 4\pi k d$, where ϵ_r is the relative permittivity, A is the effective overlap area, k is the electrostatic constant, d is the distance between electrodes. A is sensitive to shear forces and tensile strain, while d is sensitive to normal forces.^{114,120} Based on this, Boutry et al reported a capacitive-type mechanical sensor that could measure both strain and pressure, which was capable of detecting strains as small as 0.4% and pressures less than 12 Pa (Figure 5B).¹¹⁴ Capacitive-type mechanical sensors have advantages of high sensitivity,

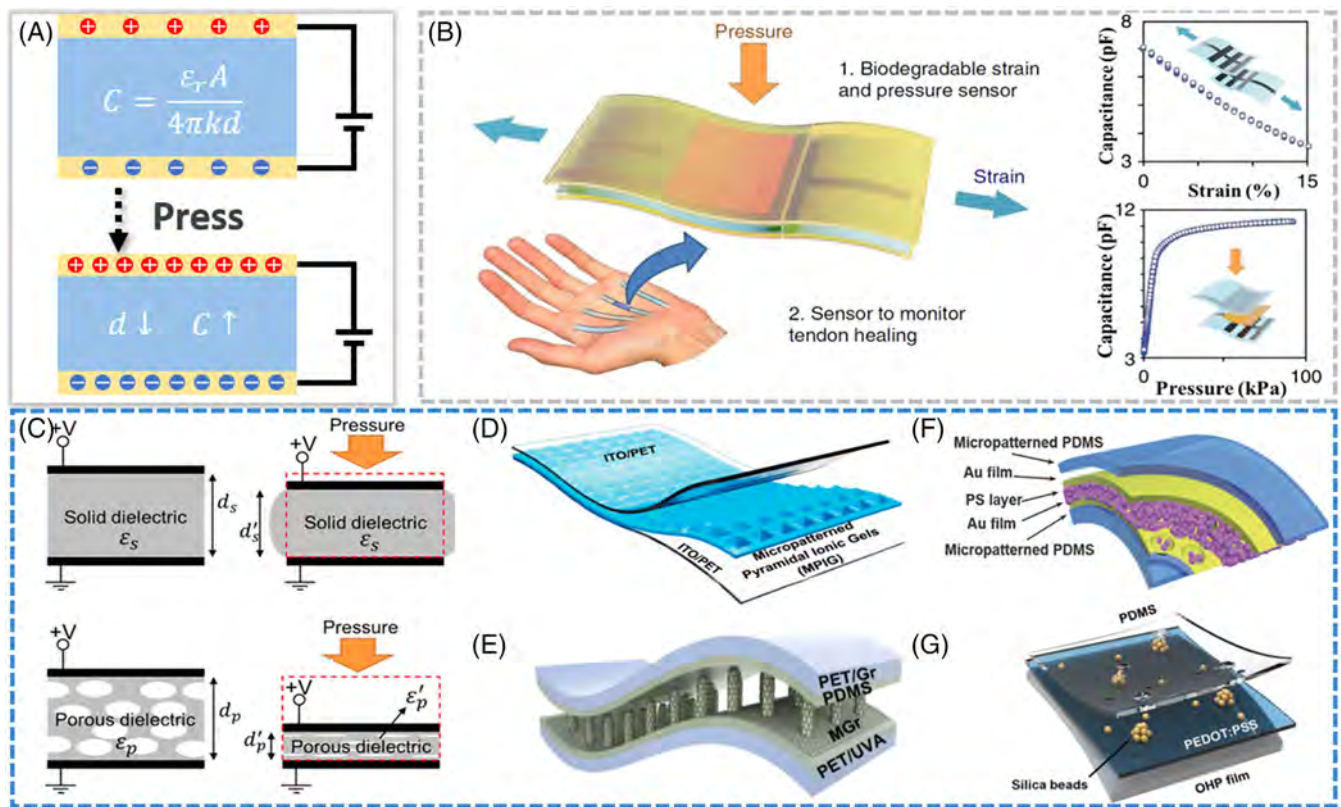


FIGURE 5 Capacitive-type mechanical sensors. A, Schematic diagram showing the working mechanism of capacitive-type mechanical sensors. B, A stretchable and biodegradable strain and pressure sensor for monitoring tendon healing.¹¹⁴ Copyright 2018, Springer Nature. C–G, Capacitive-type mechanical sensors with microstructured dielectrics: C, pores,¹¹⁵ Copyright 2016, American Chemical Society. D, Pyramids.¹¹⁶ Copyright 2017, American Chemical Society. E, Microcylinders.¹¹⁷ Copyright 2019, American Chemical Society. F, Microspheres.¹¹⁸ Copyright 2016, Wiley-VCH. G, Beads.¹¹⁹ Copyright 2018, Wiley-VCH

TABLE 1 Summary of main features of skin-inspired resistive-type mechanical sensors

Active materials	Working mode	Working range	Sensitivity	Response time (ms)	Stability	References
CNTs/leather	Pressure	<100 kPa	32.42 kPa ⁻¹ below 200 Pa, 8.03 kPa ⁻¹ at 200-1000 Pa	40	8000	80
CNT/graphene	Pressure	0.6 Pa to 6 kPa	19.8 kPa ⁻¹ below 0.3 kPa, 0.27 kPa ⁻¹ above 0.3 kPa	16.7	35 000	87
Carbonized silk nanofiber membrane	Pressure	0.8 Pa to 5 kPa	34.47 kPa ⁻¹ at 0.8-400 Pa, 1.16 kPa ⁻¹ at 400-5000 Pa	16.7	10 000	14
Microstructured graphene arrays	Pressure	1.5 Pa to 1400 Pa	5.53 kPa ⁻¹ below 100 Pa, 0.1 kPa ⁻¹ above 100 Pa	0.2	5000	108
Microstructured CNT/PDMS	Pressure	0.6 Pa- to 1200 Pa	1.80 kPa ⁻¹ below 300 Pa	10	67 500	109
Microstructured graphene	Pressure	<40 kPa	25.1 kPa ⁻¹ below 2.6 kPa, 0.45 kPa ⁻¹ above 2.6 kPa	120/80	3000	110
Graphene coated polyester fabric	Pressure	<200 kPa	8.36 kPa ⁻¹ at 0-8 kPa, 0.028 kPa ⁻¹ at 30-200 kPa	159/87	500	106
PPy hollow-sphere	Pressure	<10 kPa	7.7-41.9 kPa ⁻¹ below 100 Pa, <0.4 kPa ⁻¹ above 1 kPa	50	8000	73
PPy wrinkles	Pressure	1 Pa to 2 kPa	19.32 kPa ⁻¹ below 0.25 kPa, 0.51 kPa ⁻¹ above 1 kPa	20/30	1000	113
MXene nanosheets	Pressure	10.2 Pa to 30 kPa	0.55 kPa ⁻¹ at 23-982 Pa, 3.81 kPa ⁻¹ at 982-10 kPa, 2.52 kPa ⁻¹ at 10 to 30 kPa	11	10 000	84
Indium tin oxide	Pressure	100 Pa to 18 kPa	3.1 kPa to 1 below 6 kPa, 15.4 kPa to 1 at 6-18 kPa	0.5	6000	90
Ag NWs/silk	Strain	<50%	1-15, tunable	-	-	92
Liquid metal/PDMS	Strain	<15%	15	-	100	74
Graphene/silk fibroin	Strain	<90%	4-34, 634-470 within strain of 0%-70%, 70%-90%	-	10 000	100
Ag NPs/reduced graphene oxide	Strain	<14.5%	183, 475 within strain of 0%-8%, 8%-14.5%	-	500	88
Graphene coated polyester	Strain	<15% (x), <8% (y)	1.7 (x-direction), 26 (y-direction)	-	500	105
Carbonized silk fabric	Strain	<500%	9.6, 37.5 within strain of 0%-250%, 250%-500%	70	10 000	94
PPy/polyurethane	Strain	<1450%	0.1	500	-	81
Li+/agar/polyacrylamide	Strain	<1100%	1.8	-	100	83
MOF	Strain	2.5%-3.3%	10 000 within strain of 2.5%-3.3%	-	1000	70
MXene	Strain	<2.13%	180.1, 94.8 within strain of 0%-0.11%, 0.11%-2.13%	30	4000	85

Abbreviations: CNT, carbon nanotube; MOF, metal-organic framework; NW, nanowire; PDMS, polydimethylsiloxane; PPy, polypyrrole; NPs, nano particles.

low power consumption, and better temperature independence. However, the sensitivity of the capacitive-type sensors is limited by A , and it is sharply reduced as the size of the device decreases. Developing small area capacitive-type mechanical sensor with high sensitivity remains challenging.

Capacitive-type mechanical sensors generally consist of a dielectric layer sandwiched by two flexible electrodes. Low modulus dielectrics (eg, PDMS,²⁶ Ecoflex,¹²¹ and acrylic elastomer¹²²) are often used to increase the sensitivity of capacitive-type mechanical sensors due to their larger deformation. However, due to the incompressible

TABLE 2 Summary of main features of skin-inspired capacitive-type mechanical sensors

Active materials	Working mode	Working range	Sensitivity	Response time (ms)	Stability	References
Fingerprint-like patterned 3D graphene	Pressure	0.2 Pa to 75 kPa	110 kPa ⁻¹ below 0.2 kPa	30	10 000	15
CNT-poly(lactic acid)	Pressure	12 Pa to 430 kPa	0.7 kPa ⁻¹ under 1 kPa, 0.13 kPa ⁻¹ at 5-10 kPa	-	30 000	114
CNT/3D microporous elastomer/CNT	Pressure	0.1 Pa to 130 kPa	0.601 kPa ⁻¹ under 5 kPa, 0.077 kPa ⁻¹ at 30-130 kPa	-	1000	115
Au/polystyrene microspheres/Au	Pressure	17.5 Pa to 500 kPa	0.815 kPa ⁻¹	38	-	118
Ag NW/flower/Ag NW	Pressure	0.6 Pa to 115 kPa	1.54 kPa ⁻¹ under 1 kPa, 0.068 kPa ⁻¹ at 1-40 kPa, 0.014 kPa ⁻¹ above 40 kPa	-	5000	124
PEDOT:PSS/Nafion	Pressure	<30 kPa	5 kPa ⁻¹ below 5 kPa, 0.15 kPa ⁻¹ at 10-30 kPa	0.5	>10 000	17
PEDOT:PSS/SiO ₂ beads/PEDOT:PSS	Pressure	2 Pa to 30 kPa	1.0 kPa ⁻¹ under 2 kPa	140/110	1000	119
ITO/porous PDMS	Pressure	90 kPa	0.63 kPa ⁻¹ under 1 kPa	40	10 000	125
ITO/micropatterned pyramidal ionic gels	Pressure	10 Pa to 50 kPa	41.64 kPa ⁻¹ under 0.4 kPa	20	5000	116
polyethylene terephthalate/microconformal graphene/polyethylene terephthalate	Pressure	44 mPa to 4 kPa	7.68 kPa ⁻¹	30	600	117
Nafion hydrogel	Pressure	30 kPa	5 kPa ⁻¹ under 5 kPa, 0.15 kPa ⁻¹ at 10-30 kPa	0.5	10 000	17
CNT/poly(lactic acid)	Strain	0.4%-54%	3.33	-	20 000	114
Polyacrylamide hydrogel	Strain	1%-500%	-	-	1000	122

Abbreviations: CNT, carbon nanotube; ITO, indium tin oxide; NW, nanowire; PEDOT:PSS, poly(3,4-ethylene dithiophene):poly(styrene sulfonate); PDMS, polydimethylsiloxane; PPy, polypyrrole; PET, polyethylene terephthalate.

and viscoelastic of the elastomeric dielectrics, the sensitivity and response time of capacitive-type mechanical sensors are still limited. To address this challenge, researchers developed dielectric materials with microstructures (eg, pores,^{17,118,119} pyramids,^{121,123} microcylinders,¹¹⁷ microspheres,¹¹⁸ beads,¹¹⁹ and needles¹²⁴) (Figure 5C-G). As shown in Figure 5C, an ultralow limit (0.1 Pa) pressure sensor based on a microporous dielectric elastomer was reported.¹¹⁵ Even under very low pressure, it could still produce a considerable deformation, enhancing the sensitivity. In addition, natural materials (such as flowers and leaves) have been directly used as the dielectric layer in capacitive-type mechanical sensors.¹²⁴ These natural materials typically possess microstructured surfaces, which can improve sensitivity. They are rich in the source, low in cost, nonpolluting, and can be used on a large scale, providing a new choice for dielectric elastomers. Meanwhile,

the conductive electrode significantly affects the flexibility and stretchability of the capacitive-type mechanical sensor. For example, Sun et al combined stretchable ionic conductor with a stretchable dielectric and obtained an extremely stretchable mechanical sensor which could detect strains up to 500%.¹²² In summary, the comparison of main features between skin-inspired capacitive-type mechanical sensors based on different materials and structures is summarized in Table 2.

2.3 | Piezoelectric-type mechanical sensors

Piezoelectric-type mechanical sensors can convert dynamic pressures into electrical signals via piezoelectric materials with the advantages of high sensitivity and fast response,

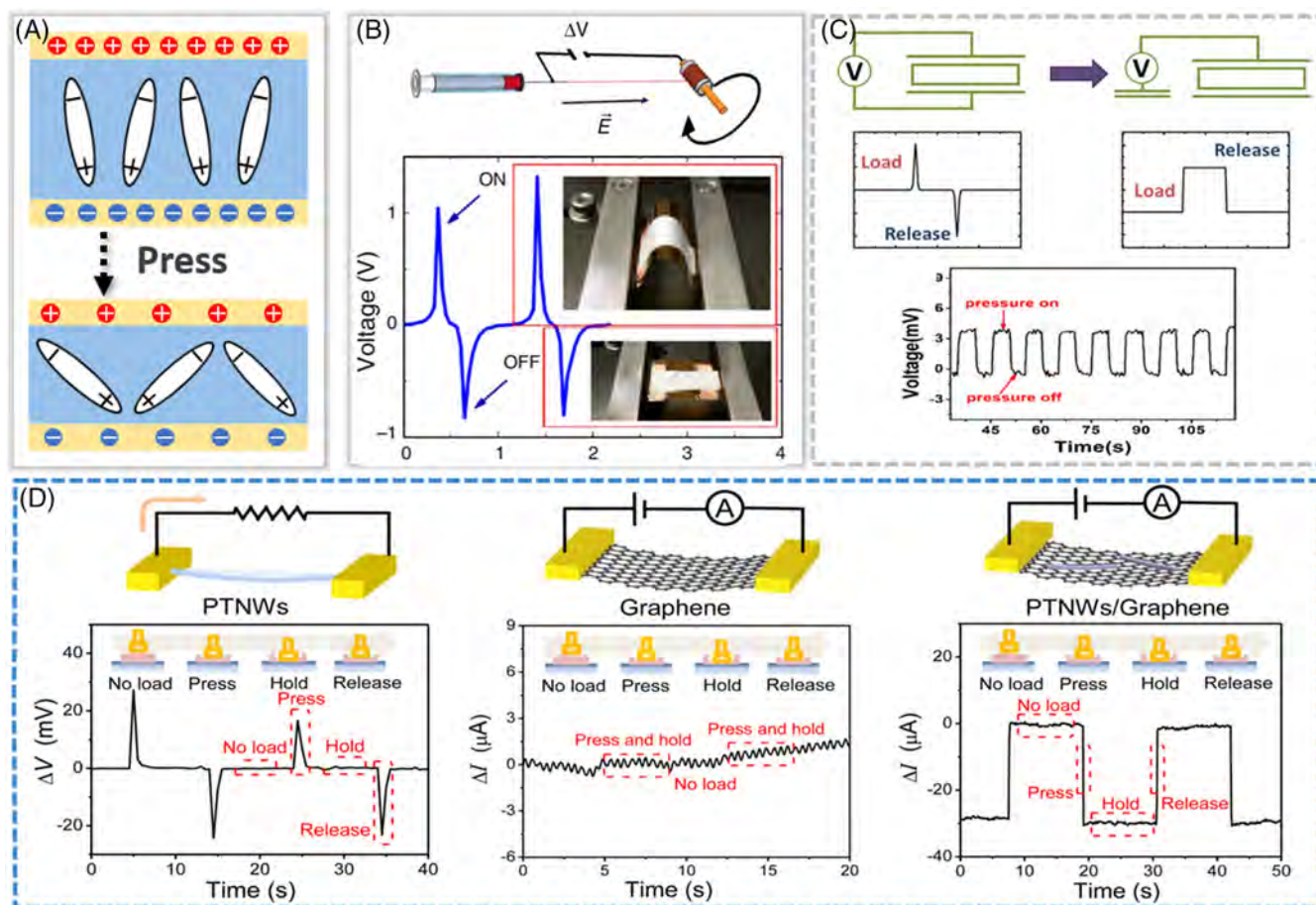


FIGURE 6 Piezoelectric-type mechanical sensors. A, Schematic diagram of piezoelectric effects. B, A high performance piezoelectric-type mechanical sensor based on aligned arrays of P(VDF-TrFE).¹²⁷ Copyright 2013, Springer Nature. C, A single-electrode piezoelectric-type mechanical sensor with a square wave electrical response.¹⁸ Copyright 2018, American Chemical Society. D, Performance comparisons of PTNWs, graphene, and PTNWs/graphene pressure sensors.¹²⁸ Copyright 2017, American Chemical Society. PTNWs, PbTiO₃ nanowires; P(VDF-TrFE), poly(vinylidene fluoride-co-trifluoroethylene)

which are widely used in dynamic monitoring.¹²⁶ Piezoelectric effect refers to the spatial separation of positive and negative charges generated by an applied force, inducing by rearrangement of dipoles (Figure 6A).¹²⁹ The intensity of the piezoelectric effect can be calculated by $q = d_{33}F$, where q is the amount of separated charge, d_{33} is the piezoelectric strain constant, and F is the applied force. Compared with capacitive-type and resistive-type sensors, piezoelectric-type sensors are self-powered and have broader application prospects. For example, Persano et al employed aligned arrays of poly(vinylidene fluoride-co-trifluoroethylene) (P(VDF-TrFE)) and fabricated a flexible, large area, and self-powered mechanical sensor with ultrahigh sensitivity even at exceptionally small pressure (0.1 Pa) (Figure 6B).¹²⁷

However, as many piezoelectric materials have pyroelectric effects, piezoelectric-type mechanical sensors need to address the challenge of thermal interference. For example, Wang et al demonstrated a new device structure that comprises a single-electrode piezoelectric generator and a capacitor, as shown in Figure 6C. The piezoelectric

signal was converted into a square wave by a capacitor, which was distinguished from the pyroelectric pulse signal. Therefore, pressure and temperature stimuli could be detected simultaneously.¹⁸

In addition, the piezoelectric-type mechanical sensors are not suitable for static sensing because of the impulsive output signal. Therefore, one challenge of piezoelectric-type mechanical sensors is to realize static pressure measurements in a simple way. For example, Chen et al developed a mechanical sensor with NWs/graphene heterostructures for static force sensing, which was based on the synergistic effects between polarization charges in PbTiO₃ NWs and changes in carrier migration in graphene (Figure 6D).¹²⁸ Compared with the conventional resistive-type and piezoelectric-type mechanical sensors, this sensor can measure both static and dynamic pressures with ultrahigh sensitivity ($9.4 \times 10^{-3} \text{ kPa}^{-1}$) and ultrafast response time (5–7 ms).

Commonly used piezoelectric materials can be divided into two categories: inorganic (eg, lead zirconate titanate,¹³⁰

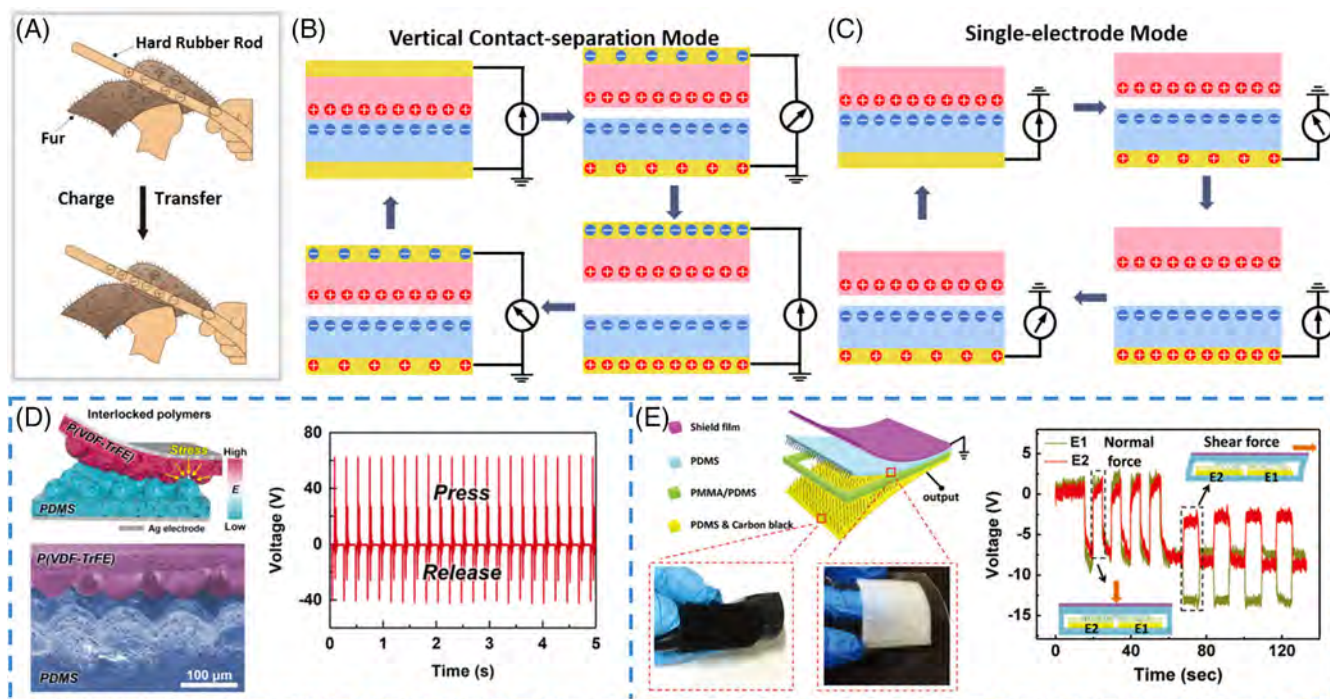


FIGURE 7 Triboelectric-type mechanical sensors. A, Schematic diagram of the triboelectric-type effect. B, Vertical contact-separation mode. C, Single-electrode mode.¹³⁶ Copyright 2018, Wiley-VCH. D, Triboelectric-type mechanical sensors with gradient stiffness.¹³⁹ Copyright 2018, American Chemical Society. E, Triboelectric-type mechanical sensors with tiny burr interlocking structures.¹⁴⁰ Copyright 2018, Wiley-VCH

ZnO,¹³¹ and BaTiO₃¹³²) and organic (eg, polyvinylidene fluoride [PVDF],¹⁸ P(VDF-TrFE)¹²⁷). Inorganic piezoelectric materials exhibit high sensitivity but low flexibility. For application in skin-inspired electronics, researchers typically disperse inorganic nanoparticles in a polymer matrix to realize flexibility.¹³³ In contrast, organic piezoelectric materials have the advantages of flexibility, lightweight, and ease of fabrication.¹³⁴ However, they exhibit lower sensitivity, so researchers often use additives to improve their performance. For example, Baur et al doubled the piezoelectric properties of PVDF by introducing carbon nanomaterials (CNTs and C₆₀).¹³⁵ Carbon nanomaterials can introduce more charge and adjust the relative dielectric constant of PVDF.

2.4 | Triboelectric-type mechanical sensors

The triboelectric-type mechanical sensor is a kind of novel self-powered sensor that converts a mechanical signal into an electrical signal through triboelectric effects. It has been intensively studied in recent years.¹³⁶⁻¹³⁸ As early as 2600 years ago, the triboelectric effect, known as contact electrification, has been discovered. Charge transfer occurs during frictional contact between different materials (Figure 7A).¹³⁶ The standard for measuring charge transfer is called triboelectric order.¹⁴¹ Similar to piezoelectric-type

sensors, triboelectric-type mechanical sensors generate electrical signals only at the moment of contact and separation. Hence, most triboelectric-type mechanical sensors are more suitable for dynamic sensing.

Triboelectric nanogenerators (TENG) are one of the most widely studied triboelectric-type mechanical sensors in recent years. Wang et al reported the first transparent TENG for self-powered pressure sensor in 2012.¹⁴² TENG can be divided into four working modes: (a) the vertical contact-separation mode; (b) the lateral sliding mode; (c) the single-electrode mode; and (d) the free-standing mode.¹⁴³ Among them, the vertical contact-separation mode¹⁴⁴⁻¹⁴⁶ and the single-electrode mode^{147,148} are the most common modes in mechanical sensors, as shown in Figure 7B,C. The output performance of TENG is affected by the magnitude and frequency of the mechanical stimuli.^{144,149} Through experimental measurements and theoretical calculations, it is found that the open-circuit voltage (V_{OC}) is linear with the applied pressure, and the short-circuit current (I_{SC}) has a linear relationship with the frequency, which provides a theoretical basis for triboelectric-type mechanical sensors.

Triboelectric-type mechanical sensors with special structures and functions have been developed to improve sensing performance. For example, Ha et al mimicked human skin and developed an interlocked microstructured composites with gradient stiffness for triboelectric-type mechanical sensors (Figure 7D).¹⁴⁵ Gradient stiffness

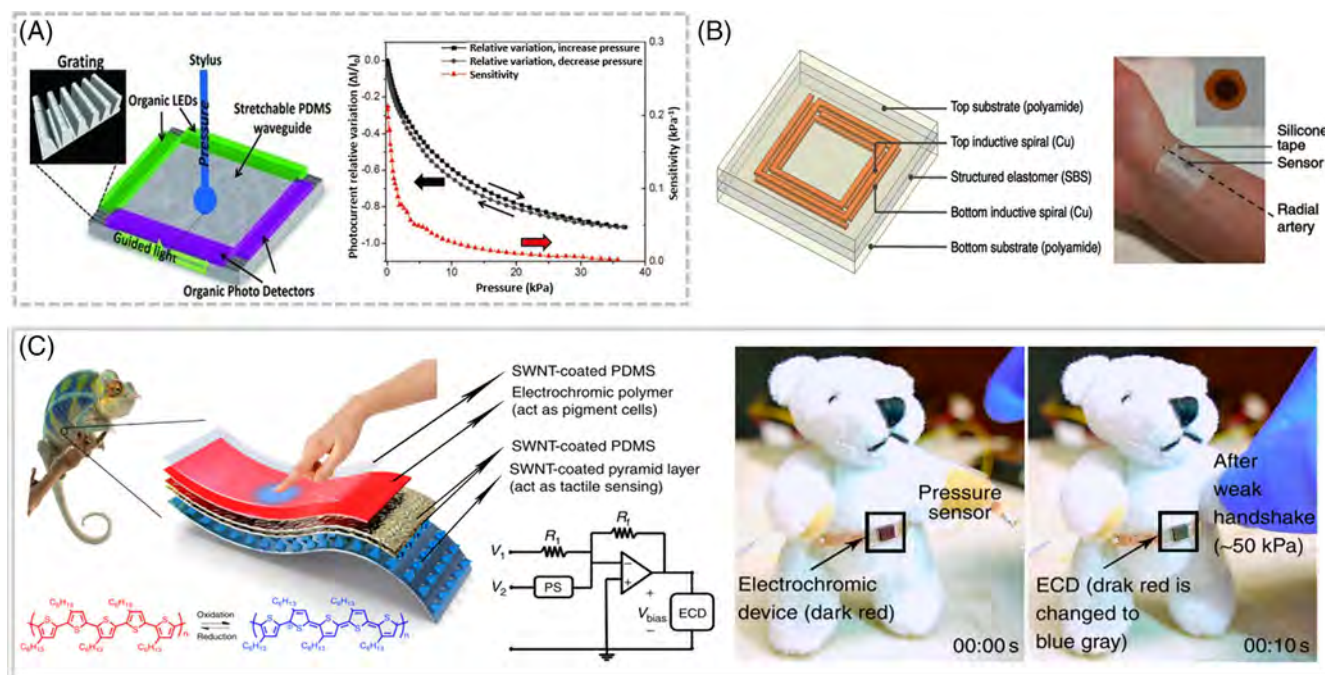


FIGURE 8 Other types of mechanical sensors. A, Optical-type mechanical sensors.¹⁵⁰ Copyright 2012, Wiley-VCH. B, Wireless-type mechanical sensors.⁶³ Copyright 2014, Springer Nature. C, Visualized (discoloration) mechanical sensors.⁶² Copyright 2015, Springer Nature

provided large contact areal differences and high compressibility, resulting in higher sensitivity (0.55 V/kPa). Ren et al developed a metal-free triboelectric-type sensor with tiny burr interlocking structures to achieve high sensitivity detection of normal force and shear force (Figure 7E).¹⁴⁰ In addition, encapsulated in PET protective layers, the sensor achieved good waterproofness and can sustain harsh environments such as rain or underwater.¹⁴⁶

2.5 | Other types of mechanical sensors

In addition to the above sensors, other types of mechanical sensors have been investigated. Recently, optical-type mechanical sensors have attracted interest because they do not interfere with other electronic signals and have the potential for large-area applications (Figure 8A).¹⁵⁰ In addition, stress can induce changes in the resonant frequency. Based on this, Chen et al developed a wireless-type pressure sensor with potential in the field of health monitoring (Figure 8B).⁶³ Also, conversion of mechanical signals into visualized optical signals has attracted wide attention. Combining electroluminescent materials or aggregation-induced emission materials with mechanical sensors, mechanical signals can be converted into changes in electrical signals (eg, capacitance,^{16,116,151} resistance,⁶²) or concentration of materials,¹⁴⁵ which can further lead to changes in color (Figure 8C).

3 | SKIN-INSPIRED TEMPERATURE SENSORS

Detecting temperature is another important function of human skin, which can recognize temperature changes as small as 0.02°C.¹⁵¹ Body temperature is a key indicator for monitoring human activities and health. For example, an abnormal increase in body temperature may be associated with inflammation or fever. Therefore, body temperature can be used as an auxiliary diagnostic basis for some diseases (eg, cardiovascular disease, cancer).¹⁰ In addition, the human body can adjust body temperature by regulating the balance between heat generation and heat dissipation.

Inspired by human skin, researchers have developed flexible, stretchable, and biocompatible temperature sensors. According to the working mechanisms, temperature sensors can be divided into resistance-type temperature detectors (RTDs),¹⁵² thermistors,¹⁵³ pyroelectric-type temperature sensors,¹⁵⁴ thermoelectric-type temperature sensors,¹⁵⁵ and so on. The details of skin-inspired temperature sensors are reviewed in this section.

3.1 | Resistance-type temperature detectors

RTDs are one kind of the most commonly used temperature sensors, which have high linearity, wide working range, and high stability.¹⁵⁶ The temperature signal is

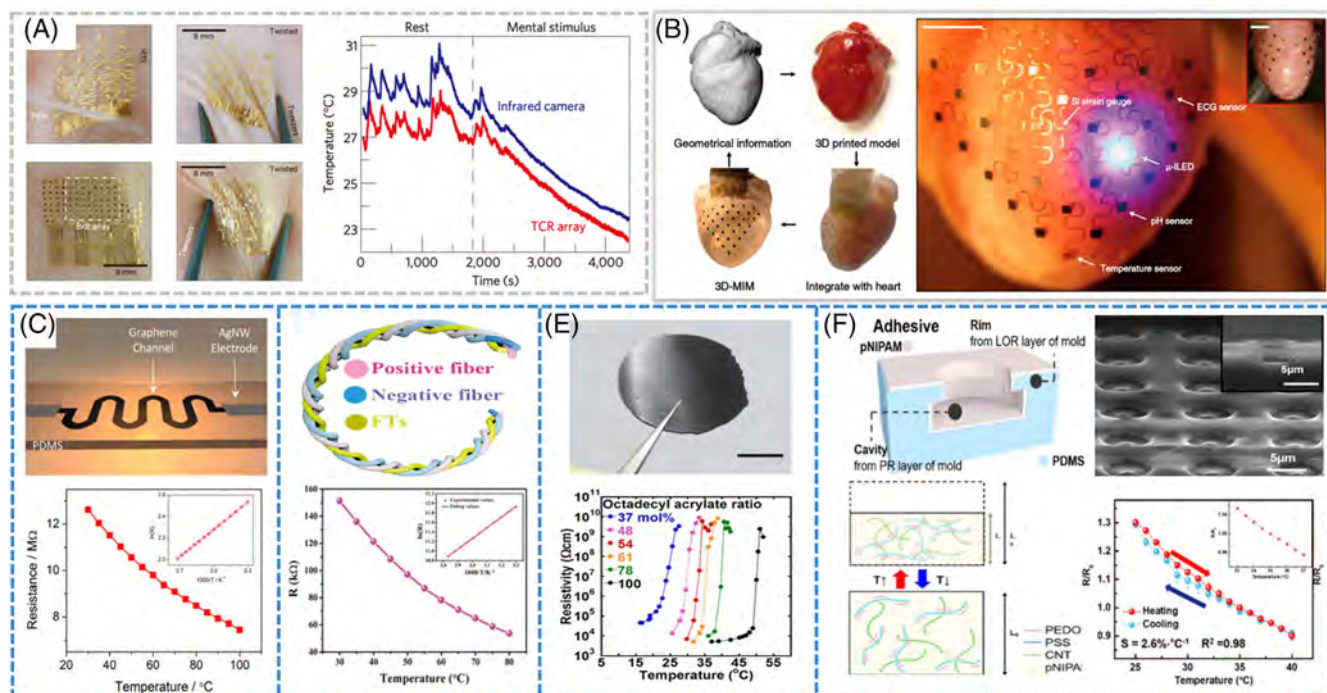


FIGURE 9 Resistance-type temperature detectors and thermistors. A, Ultrathin, conformal and stretchable Au-based RTDs.²⁰ Copyright 2013, Springer Nature. B, Implantable RTD for spatiotemporal cardiac measurements, scale bar, 2 cm.¹⁵⁹ Copyright 2014, Springer Nature. C, Stretchable graphene thermistor.¹⁶⁰ Copyright 2015, American Chemical Society. D, 3D printing GO fiber thermistor.¹⁶¹ Copyright 2018, Wiley-VCH. E, Ultrahigh sensitive PTC polymer thermistor.¹⁶² Copyright 2015, National Academy of Sciences. F, Adhesive temperature sensor (mimicking octopus suction cups).¹⁶³ Copyright 2018, American Chemical Society. GO, graphene oxide; PTC, positive temperature coefficient; RTDs, resistance-type temperature detectors

converted into an electrical signal based on the dependence of the resistance on the temperature. The temperature coefficient of resistance (TCR) is a key indicator for evaluating the sensitivity of RTDs, which can be calculated by $TCR = (1/R_0) \cdot (\Delta R/\Delta T)$, where ΔR is the change of the resistance, R_0 is the original resistance, and ΔT is the change of the temperature.

Metal materials (eg, Pt,^{23,157} Au,^{20,159} Ag,^{152,200,247} and Mg¹⁵⁸) are conventional active materials used in RTDs. RTDs for medical monitoring have been paid more and more attention. In order to achieve precise and continuous thermal characterization of the human body, it is necessary to develop ultrathin, conformal, and stretchable RTDs (Figure 9A).²⁰ Moreover, developing implantable temperature sensors is the next goal for electronic skin applications. For example, researchers integrated an Au-based RTD with semiconducting metal oxides and developed implantable detector arrays that can detect heart temperature, strain, and pH in real time (Figure 9B).¹⁵⁹

3.2 | Thermistors

Thermistors are also a kind of commonly used temperature sensors that convert temperature changes into

resistance changes. Compared to the RTDs, the thermistors have the advantages of high sensitivity and short response time.¹⁶⁴ The sensitivity index of thermistors is defined by $B = (E_a/2k)$, where B is thermal index, E_a is activation energy, while k is Boltzmann constant. Thermistors can be classified into two types: negative temperature coefficient thermistors and positive temperature coefficient (PTC) thermistors.

Transition metal oxide (eg, NiO, CoO, and MnO) semiconductors and perovskite crystals (eg, BaTiO₃, SrTiO₃, and PbTiO₃) are commonly used materials for thermistors.^{164,165} However, these materials are generally rigid, which limits their applications in skin-inspired electronics. Therefore, it is highly desired to develop flexible and stretchable thermistors. Recently, flexible thermistors based on different kinds of materials (eg, graphene,^{160,161,166} CNTs,⁴⁰ conductive polymers,²¹ and their composites^{153,162,163,167-170}) have been explored (Figure 9C-F). Generally, the sensitivity of thermistors can be further improved by the synergistic effect of two activity materials (eg, PEDOT:PSS/graphene,¹⁶⁷ PEDOT:PSS/CNTs,¹⁶³ and graphene/PU^{170,171}). For example, Jeon et al developed Ni microparticle-filled binary polymer composites as temperature sensors with ultrahigh sensitivity, which are attributed to the transformation of the crystalline phase to the amorphous phase.¹⁶⁹ The phase transition

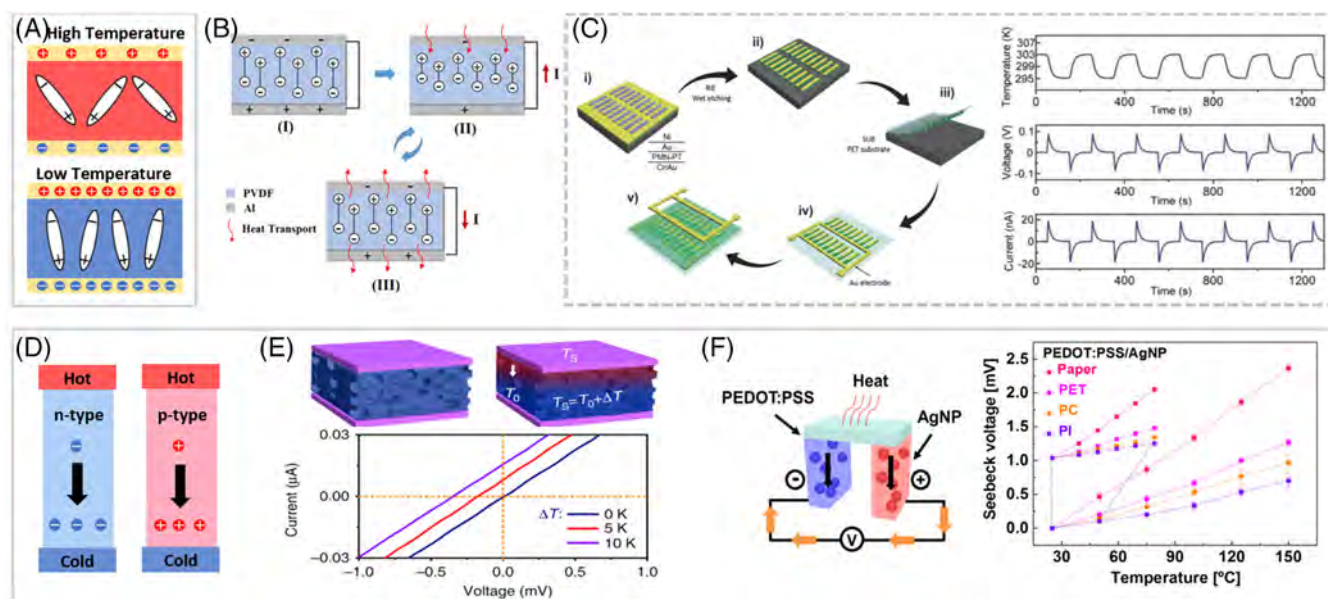


FIGURE 10 Pyroelectric-type and thermoelectric-type temperature sensors. A, Schematic diagram of pyroelectric effect. B, PVDF pyroelectric-type temperature sensors for respiratory monitoring.¹⁷² Copyright 2017, Elsevier. C, PMN-PT ribbon-based piezoelectric-pyroelectric temperature sensors.¹⁷³ Copyright 2017, Wiley-VCH. D, Schematic diagram of thermoelectric effect. E, Illustrative schematic and electrical properties of thermoelectric temperature sensors.¹⁷⁴ Copyright 2015, Springer Nature. F, Paper-based thermoelectric-type temperature sensors.¹⁵⁵ Copyright 2017, American Chemical Society. PMN-PT, $(1-x)\text{Pb}(\text{Mg},\text{Nb})\text{O}_3\cdot x\text{PbTiO}_3$; PVDF, polyvinylidene fluoride

resulted in large volume expansion and the increased distance between the conductive particles.

Temperature sensors for health monitoring require a high sensitivity within a temperature range to body temperature. Yokota et al reported an ultraflexible and printable temperature sensor based on acrylate polymers and graphite, which exhibited changes in resistivity by six orders of magnitude for a change in temperature of only 5°C (Figure 10E).¹⁶² The most sensitive temperature range was adjustable within 25°C to 50°C by changing the mixing ratio of the two acrylate monomers, covering all physiological meaningful temperature ranges. In addition, inspired by the octopus tentacle structure, Oh et al developed a micro-patterned temperature sensor with excellent adhesion properties for medical and health care monitoring (Figure 10F).¹⁶³

3.3 | Pyroelectric-type temperature sensors

Pyroelectric-type temperature sensors can convert a temperature signal into a voltage signal.^{175,176} Unlike resistive-type temperature sensors, they are self-powered. The sensing capability of pyroelectric-type temperature sensors originated from the pyroelectric effect, which relates to the changes of polarization of a spontaneously polarized crystal with temperature (Figure 10A).

Pyroelectric effects are widespread in ceramic crystals^{177,178} and polymers.¹⁷⁹ The open-circuit voltage of pyroelectric-type temperature sensors can be calculated by the formula: $V_{\text{pyro}} = k \cdot (p/\epsilon_{33}^T) \cdot h \cdot \Delta T$, where k is a constant, p is the pyroelectric coefficient, ϵ_{33}^T is the permittivity, h is the thickness, and ΔT is the change in temperature.^{6,180}

Pyroelectric polymers (eg, PVDF,¹⁷² P(VDF-TrFE)¹⁸¹) are widely used in skin-inspired electronics due to their excellent flexibility and stability. Pyroelectric polymers with a low crystallinity have negative pyroelectricity, which originates from electric dipoles oscillate within a larger degree at high temperature that results in a decrease of the spontaneous polarization strength.¹⁸² On the contrary, highly crystalline pyroelectric polymers have positive pyroelectricity due to their large residual polarization.¹⁸³ Based on the pyroelectric effect of PVDF, Xue et al prepared a self-powered temperature sensor for respiratory monitoring (Figure 10B).¹⁷² In addition, researchers used the enhanced electrophysical coupling effects of nanocomposites to improve the stability and achieved multiple functions.^{154,173,184,185} For example, Chen et al fabricated a pyroelectric temperature sensor with micropatterned $(1-x)\text{Pb}(\text{Mg},\text{Nb})\text{O}_3\cdot x\text{PbTiO}_3$ (PMN-PT) ribbons, which showed excellent piezoelectric and pyroelectric properties (Figure 10C).¹⁷³ Moreover, studies have shown that the pyroelectric effect of nanocomposites (P(VDF-TrFE)/BaTiO₃) can be easily tuned by adjusting the content, resulting in a controllable sensitivity of pyroelectric-type temperature sensors.¹⁵⁴

3.4 | Thermoelectric-type temperature sensors

Thermoelectric-type temperature sensors are another kind of self-powered temperature sensors, which can convert temperature signals into voltage signals based on the thermoelectric effect.^{175,186,187} The thermoelectric effect refers to a phenomenon in which current or charge is generated when carriers (electrons and holes) move with a temperature gradient (Figure 10D). The generated voltage is defined as $V_{\text{therm}} = S_e \cdot \Delta T$, where S_e is the Seebeck coefficient and ΔT is the difference in temperature.

The thermoelectric effect is widely present in semiconductors¹⁸⁸ and conductors,¹⁸⁹ wherein the effect of semiconductors is more pronounced. In recent years, some new thermoelectric materials (eg, organic semiconductors,^{174,248} conductive polymers,¹⁹⁰⁻¹⁹² graphene,¹⁹³ and CNTs^{194,195}) have received extensive attention. Based on organic thermoelectric materials (PEDOT:PSS), Zhang reported a flexible temperature sensor with an accurate resolution of 0.1 K (Figure 10E).¹⁷⁴ Furthermore, Hou et al developed an all-graphene electronic skin based on thermoelectric effects of graphene, which can monitor both temperature and mechanical stimuli.¹⁹⁶ Jung et al fabricated a paper-based thermoelectric-type temperature sensor using PEDOT:PSS and Ag nanoparticles, which exhibited temperature-sensing capability over a wide range (20–150°C) (Figure 10F).¹⁵⁵ Higher sensitivity and faster response can be achieved through the coupling of two thermoelectric materials. For example, Yang et al reported a temperature sensor based on a graphene/CNT composite, which was highly responsive to a subtle temperature gradient.¹⁹⁷ In addition, the thermoelectric materials can also supply power for other sensors in the skin-inspired electronics.¹⁹⁸

In addition to the above sensors, skin-inspired temperature sensors with novel structures or properties have been reported. For example, temperature sensors with special structures can exhibit special performance. Park et al mimicked the human fingertip and created interlocked microstructures in the temperature sensor to increase the TCR.¹⁸⁵ Ota et al demonstrated a highly deformable liquid-state heterojunction temperature sensor, presenting a significant advance in the development of liquid-state electronics.¹⁹⁹

In conclusion, the comparison of main features between skin-inspired temperature sensors based on different working mechanisms and materials are summarized in Table 3.

4 | SKIN-INSPIRED HUMIDITY SENSORS

Humidity (environmental humidity, hydration of skin) is also an extremely important indicator, which plays an

important role in human physiological activity. Monitoring of skin hydration can be used to diagnose skin diseases and measure treatment effects. Moreover, detecting environmental humidity is also very important, people who work or live in high-temperature and high-humidity environments are prone to heatstroke. Although it does not contain a humidity detector, the skin can still respond to wetness through mechanoreceptors and thermal receptors.²⁰¹ In addition, the skin can adjust its moisture by sweating to ensure the normal progress of physiological activities.

Several sensors for measuring humidity have been developed, which can sense humidity by measuring changes in physical parameters.^{202,203} However, these sensors are usually bulky and rigid, limiting their applications in monitoring skin humidity in real time. Therefore, there is an urgent demand to develop lightweight, flexible, and stretchable humidity sensors that can be integrated into skin-inspired electronics. According to the working mechanism, humidity sensors can be divided into resistive-type sensors,^{27,207-210} capacitive-type sensors,^{23,25,26,211,212} moisture-dependent power generators,²⁰⁴⁻²⁰⁹ and so on. The details of humidity sensors for skin-inspired electronics are presented in this section.

Resistive-type humidity sensors are one kind of the most commonly used humidity sensors for skin-inspired electronics. The resistivity of an active material generally changes with humidity. For example, the resistance of the carbon nanocoils decreases as the humidity increases. Based on this effect, Wu et al used carbon nanocoils to fabricate a resistive-type humidity sensor with excellent sensing performance, including a fast-response (1.9 seconds), wide relative humidity (RH) broad range (4%–95%), highly sensitive (0.8% RH), and remarkable stability (Figure 11A).²¹⁰ Wang et al demonstrated a reduced graphene oxide (rGO) film prepared by an exfoliation method at the liquid/air interface, which exhibited a negative resistance response. When exposed to humid air, the rGO sheets will adsorb water molecules and ionize hydronium ions (H_3O^+), resulting in a decrease in resistivity.²¹²

Capacitive-type humidity sensors are also widely studied in recent years, which convert humidity signals into capacitance changes. Humidity can regulate the capacitance by affecting the dielectric constant of the air. Capacitive-type humidity sensors exhibit the advantages of simple structure, high repeatability, and low requirements on active materials. The capacitance between the GO sheets increases with the increasing humidity.²⁶ As shown in Figure 11B, Zhao et al prepared capacitive-type humidity sensors using graphene woven fabrics and films on different supporting materials (PDMS, cellulose acetate butyrate), indicating that the state of graphene and the type of supporting materials both influenced the change of capacitance.²¹¹

TABLE 3 Summary of main features of skin-inspired temperature sensors

Active materials	Working mechanism	Working range (°C)	Sensitivity (°C ⁻¹)	References
Au	RTD	10-85	0.028%	20
Ag	RTD	25-50	0.17%	200
Mg	RTD	20-50	0.20%	158
Ag NWs/polyimide	RTD	-20-20	0.31%	152
Reduced graphene oxide	RTD	0-100	0.55%	26
Graphene/silk fibroin	RTD	20-50	2.09%	100
Graphene	Thermistor	20-60	4.00%	166
Polyaniline	Thermistor	15-45	1.00%	21
CNT/PEDOT:PSS	Thermistor	25-40	2.60%	163
GO/polyurethane	Thermistor	30-80	0.80%	171
CNT/V ₂ O ₅ /vanadium nitride	Thermistor	30-80	1.95%	161
Graphite/acrylate	Thermistor	29.8-37	10 ⁵	162
Ni/polymers	Thermistor	30-40	10 ⁶ -10 ⁷	169
(1 - x)Pb(Mg,Nb)O ₃ - xPbTiO ₃	Pyroelectric	22-30	12.5 mV	173
CNT/polyaniline	Thermoelectric	-25-25	28.7 μV	194
CNT/graphene	Thermoelectric	26-40	45.3 μV	197
CNT/PEDOT:PSS	Thermoelectric	25-150	20 uV	155
PEDOT:PSS/poly(3-hexylthiophene)/ poly(2,5-bis(3-tetradecylthiophen-2-yl) thieno[3,2-b]thiophene)	Thermoelectric	0-100	35.5 μV	174

Abbreviations: CNT, carbon nanotube; GO, graphene oxide; NW, nanowire; PEDOT:PSS, poly(3,4-ethylene dioxythiophene):poly(styrene sulfonate); P3HT, poly(3-hexylthiophene); PBTBT, poly(2,5-bis(3-tetradecylthiophen-2-yl)thieno[3,2-b]thiophene); RH, relative humidity; RTD, resistance-type temperature detector; VN, vanadium nitride.

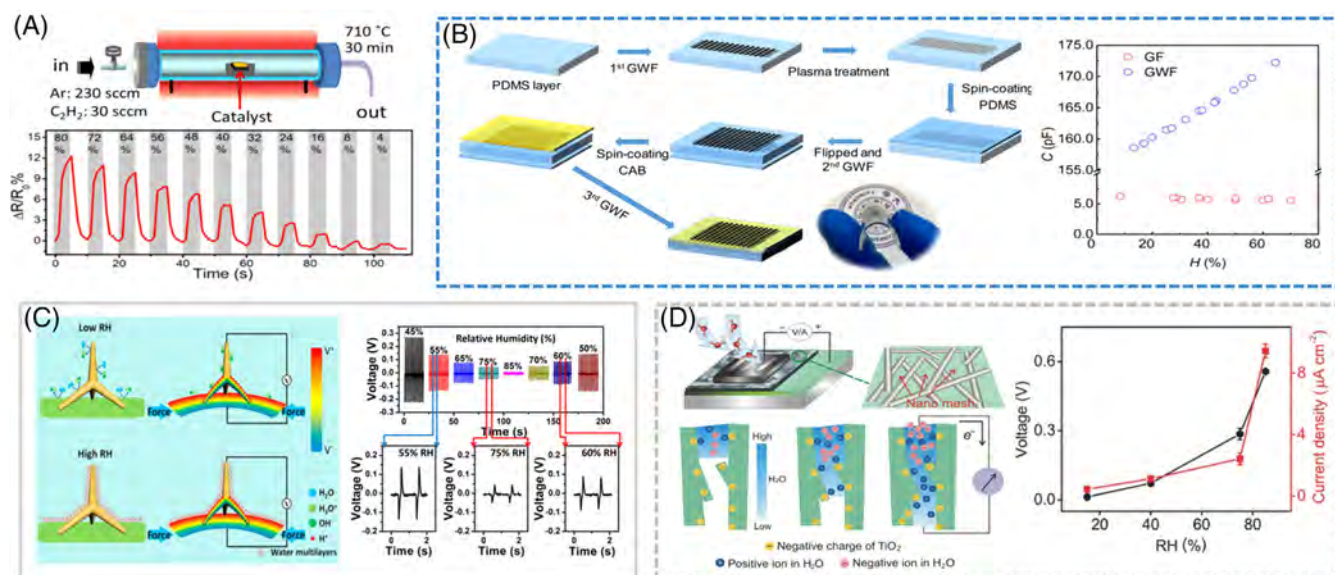


FIGURE 11 Humidity sensors. A, Resistive-type humidity sensor.²¹⁰ Copyright 2019, American Chemical Society. B, Capacitive-type humidity sensor.²¹¹ Copyright 2017, American Chemical Society. C, Moisture-dependent piezoelectric humidity sensor.²⁰⁶ Copyright 2017, Elsevier. D, Moisture-electric power generator.²⁰⁸ Copyright 2018, Wiley-VCH

In addition to the above mechanisms, humidity has a significant impact on the voltage signals generated by TENG and piezoelectric generators. Based on this, several

self-powered humidity sensors have been developed. In dry air, a voltage signal is generated when the piezoelectric material is applied with bending. But in humid air, water

molecules can be absorbed on the surface of piezoelectric materials, which can lead to the piezoelectric polarization charges and produce a low output voltage (Figure 11C).²⁰⁶

Furthermore, humidity can also generate electricity. For example, Shen et al demonstrated a TiO₂ NW humidity sensor based on the generation of electricity from ambient humidity.²⁰⁷ While diffusion along TiO₂ nanochannels, the water molecules ionized into H⁺ and OH⁻. The movement of the OH⁻ was hindered due to the negative charge of TiO₂, resulting in a separation of positive and negative charges (Figure 11D). This process is correlated to ambient humidity and thus can be used to monitor humidity.²⁰⁸ In addition, GO with gradient oxygen-containing groups, which can also generate electricity by absorbing water molecules, has also been used in humidity sensors.^{209,213,214} Several methods, including moisture-electric annealing, gradient laser reduction, and gradient thermal reduction, have been developed for preparing GO with an oxygen-containing group gradient.^{209,215-218}

In general, high-performance humidity sensors require sensing materials with large specific surface area and excellent intrinsic properties, which requires that the active material can interact with water molecules in short response time and result in great changes in certain properties. Based on this, a variety of new materials (eg, carbon dots,²¹⁹ CNTs,²²⁰ graphene,^{221,227} transition metal dichalcogenides^{27,228} hydrogels,²²² and polyelectrolytes^{223,224}) have been explored to improve the sensing performance of humidity sensors. Low-dimensional material-based humidity sensors are expected to have high sensitivity and fast response time due to the exposure of most of their atoms to the surface. For example, Zhao et al reported a single-layer molybdenum disulfide humidity sensor with ultrahigh sensitivity of more than 10⁴.²⁷ The presence of a large number of hydrophilic

groups on the active material made it easy to absorb water molecules, resulting in low detection limit. Li et al prepared a highly flexible porous ion membrane fabricated from PVA/KOH polymer gel electrolyte, which exhibited a good humidity response due to its rich hydrophilic group.²²² Furthermore, special structures have been developed to achieve better humidity sensing performance. For example, Dai et al synthesized the moisture-sensitive polyelectrolyte on the PDMS by a thiol-ene click reaction. Due to the rigid hydrophobic framework and proper hydrophilic structure, this humidity sensor exhibited an ultrafast response and high stability.²²⁴

In summarize, the comparison of main features between skin-inspired humidity sensors based on different working mechanisms and materials are shown in Table 4.

5 | NOVEL PROPERTIES OF SKIN-INSPIRED PHYSICAL SENSORS

Practical applications put forward higher demands for skin-inspired physical sensors, such as higher sensitivity, lower detection limit, wider working range, and faster response speed. In addition to the traditional performance demands, physical sensors with novel properties, such as versatility,^{226,231} self-healability,^{227,249} implantability,²²⁸ recyclability,^{200,250} and absorbability,²²⁹ are receiving more and more attention.

5.1 | Multifunctional physical sensors

Human skin can detect a variety of external stimuli. It is also necessary to develop physical sensors that are able to simultaneously detect multiple signals.

TABLE 4 Summary of main features of skin-inspired humidity sensors

Active materials	Working mechanism	Working range (RH/%)	Sensitivity (/%)	Response time (s)	References
Graphene/silk fibroin	Resistive	10-85.1	0.03%	3/6	100
GO	Resistive	4.3-75.7	0.07%	1.4/10	212
Carbon nanocoil	Resistive	4-95	0.15%	1.9/1.5	210
Polyelectrolyte	Resistive	10-95	100	0.29/0.47	224
Tungsten disulfide	Resistive	20-90	332.9	5/6	225
Ionic membrane	Resistive	6.3-95	0.79%	0.4/2.6	222
Graphene woven fabrics	Capacitive	20-70	0.19%	120/100	211
GO	Capacitive	20-90	39.23	-	26
GO	Hydroelectric generator	20-80	2.67 mV	4.5/5.5	205
TiO ₂	Hydroelectric generator	15-80	9.23 mV	-	208
TiO ₂	Hydroelectric generator	20-90	7 mV	4.5/2.8	207
Polytetrafluoroethylene	Triboelectric nanogenerator	20-100	312.5 mV	-	204

Abbreviations: GO, graphene oxide; NW, nanowire; RH, relative humidity.

Skin-inspired multifunctional sensors, which can detect various stimuli, have been reported. However, due to the mutual interferences of different stimuli, it remains challenging to fabricate multifunctional skin-inspired physical sensors. Wang et al assembled silk-derived mechanical sensors and temperature sensors into dual-mode electronic skin for the simultaneous detection of temperature and mechanical signals (Figure 12A).²³⁰ Continuous carbonized silk nanofiber membranes were used as active materials of temperature sensors, while fractured carbonized silk nanofiber membranes were used for mechanical sensors. Based on these dual-mode physical sensors, it can be used to detect and distinguish exhaling and finger pressing, which is impossible with single-mode sensors. Zhang et al reported an origami hierarchical sensor array written with GO and dopamine ink (Figure 12B),²³¹ which can simultaneously detect and distinguish complex stimuli, due to its unique time-space-resolved properties.

In addition, skin-inspired multifunctional sensors, which can simultaneously detect physical stimuli and chemical stimuli, have also been studied. For example, Nakata et al fabricated a multifunctional flexible sensor array, which can be used to simultaneously monitor skin temperature and sweat pH (Figure 12C).²³² The temperature sensor can be used to compensate for temperature-induced pH measurement errors.

5.2 | Self-healable physical sensors

Wearable physical sensors are suffering from mechanical damage due to long-term corrosion, wear, and accidental cutting, which can lead to device failure. In contrast, human skin has a strong self-healing ability. After being damaged, the skin can restore its original properties and functions by itself. Mimicking human skin, researchers have developed devices with self-healing capability to repair mechanical damage and restore sensing functions.²²⁷ The mechanisms of self-healing can be divided into two categories: self-healing by releasing healing agents (extrinsic self-healing) and self-healing by the reorganization of matrix and regeneration of dynamic chemical bonds (intrinsic self-healing).²³³ However, the healing agent is limited and it only allows limited cycles of healings in extrinsic self-healing systems.²³⁴ Therefore, intrinsic self-healing sensors have attracted significant attention.

Self-healable mechanical sensors have been widely studied. In 2012, Tee et al first reported the repeatable self-healable mechanical sensor based on a composite of supramolecular and μ -Ni microparticles (Figure 13A).⁷⁶ There were a large number of hydrogen bonds in the composite system, and the sensor achieved self-healing by the dynamic association and dissociation of these hydrogen bonds. The system can achieve rapid electrical

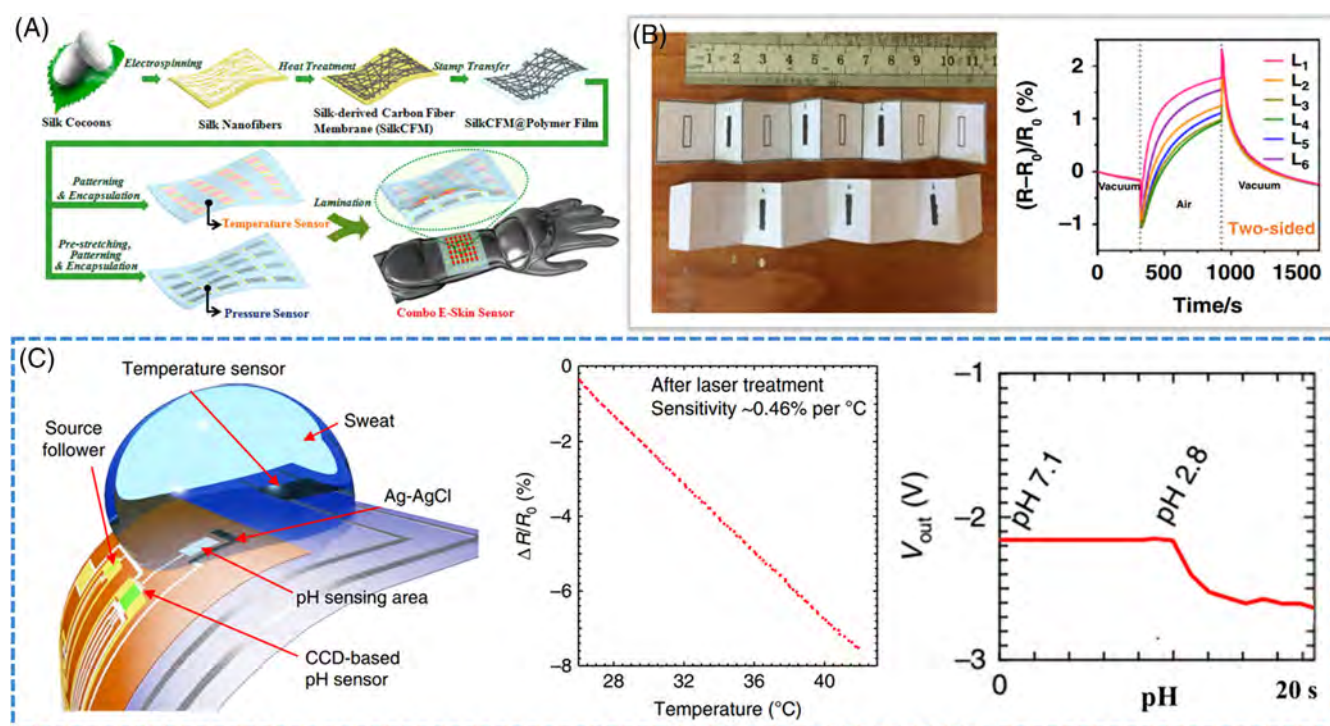


FIGURE 12 Multifunctional skin-inspired sensors. A, Silk-derived mechanical and temperature dual-mode sensor.²³⁰ Copyright 2017, American Chemical Society. B, Time-space-resolved origami hierarchical sensor array.²³¹ Copyright 2019, Springer Nature. C, Temperature sensor integrated with pH sensor.²³² Copyright 2018, Springer Nature

healing in 15 seconds, but if the fracture interfaces are exposed to air (even less than a few minutes), the healing behavior will be significantly affected. To address this problem, Wang et al developed a self-healing material with high mechanical properties and high stability based on GO and hydrogen-bonded polymer, which could maintain more than 90% self-healing efficiency after the fracture interfaces exposed to air for 24 hours.²³⁷

However, as the self-healing materials mentioned above are based on dynamic weak chemical bonds, they generally have a lower elongation at break and fracture toughness (100 J m^{-2}). Therefore, Kang et al demonstrated a self-healable polymer with extremely high stretchability (1200%) and toughness ($12\,000 \text{ J m}^{-2}$) by designing supramolecular polymers cross-linked with strong and weak hydrogen bonds (Figure 13B).²³⁵ Additionally, the hydrophobicity of the polymer backbone (PDMS) imparted the ability of self-healing in water or sweat. Based on this polymer and liquid metal, they fabricated a self-healable capacitive-type strain sensor. In addition, they embedded a CNT network in a dynamic supramolecular cross-linked polymer matrix to prepare wearable and self-healable strain, ECG sensors, and light-emitting capacitors.¹⁶ In order to achieve self-healing in complex environments (water, salt, acid, and alkaline), Cao et al developed a composite material of fluorocarbon elastomer and fluorine-rich ionic liquid for mechanical sensors and printed circuit boards. The self-healing property under various conditions is due to the stability of the fluoropolymer (Figure 13C).²³⁶

In addition to mechanical sensors, there are some other self-healable physical sensors. For example, based on thermal-sensitive fluids and supramolecular elastomer, He et al fabricated a self-healable temperature sensor.²³⁸ In addition, self-healable and multifunctional physical sensors have been developed. Wang et al reported a multifunctional and self-healable electronic skin based on graphene and silk, which can sense various physical signals such as tactile, temperature, and humidity (Figure 13D).¹⁰⁰

5.3 | Implantable physical sensors

Implantable physical sensors are a promising direction in flexible electronics. Implantable sensors can directly measure the physiological activities of organs and tissues. The primary requirement for implantable electronics is biocompatibility to avoid immune responses. They also require biodegradability or long-term stability under physiological conditions for different purposes. Biodegradable implantable electronic devices can reduce secondary damage of extraction surgery after the completion of medical function. In addition, biodegradable electronic materials can significantly reduce the environmental pollution of electronic waste.

Recently, various biocompatible materials have been reported. Some synthetic polymers (eg, silicon, polylactic acid, and PVA) and natural materials (eg, silk) are used as insulating supporting materials or sacrificial layers.²³⁹ PDMS is used by the National Heart, Lung, and Blood

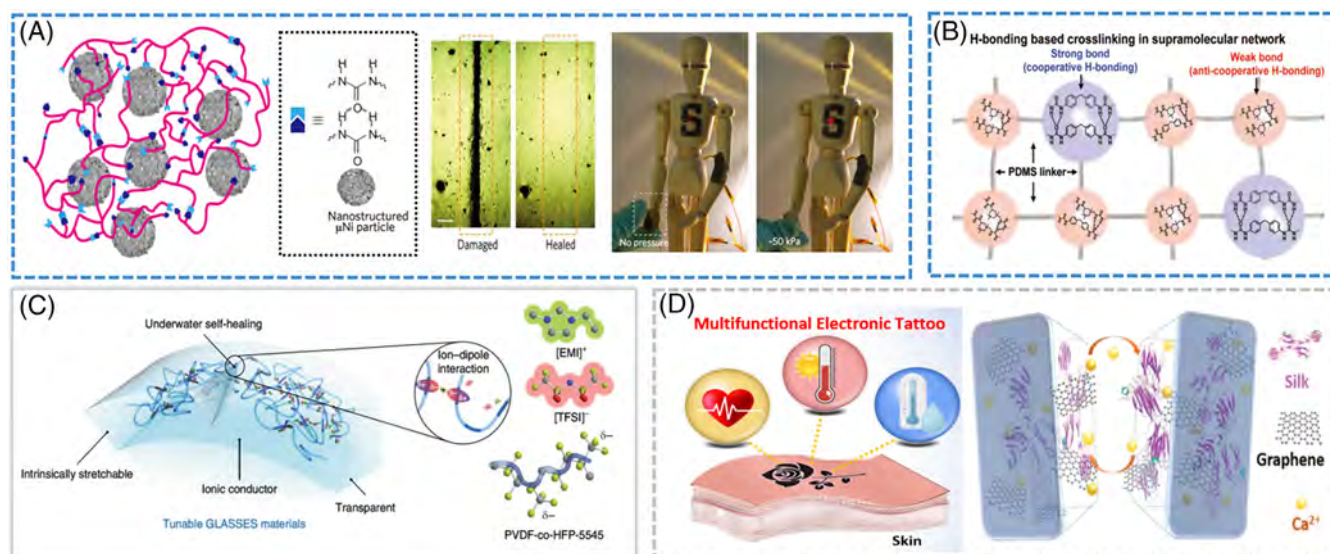


FIGURE 13 Self-healable skin-inspired physical sensors. A, Self-healable mechanical sensor (hydrogen bonds).⁷⁶ Copyright 2012, Springer Nature. B, Self-healable polymers with extremely high stretchability and toughness.²³⁵ Copyright 2018, Wiley-VCH. C, Self-healable electronics under complex environments (water, salt, acid, and alkaline).²³⁶ Copyright 2019, Springer Nature. D, Self-healable multifunctional electronic tattoo (mechanical, temperature, and humidity).¹⁰⁰ Copyright 2019, Wiley-VCH

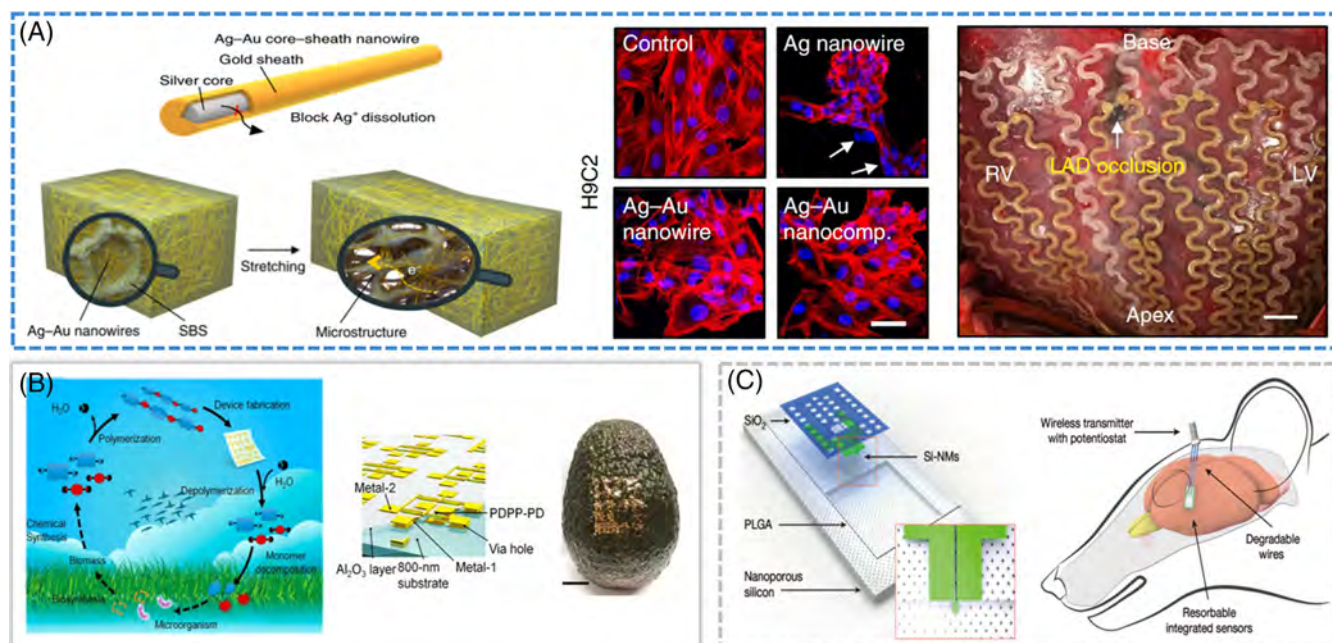


FIGURE 14 Biocompatible and biodegradable skin-inspired physical sensors. A, Biocompatible active material (Ag-Au nanowire) for the implantable electrophysiological sensor (Scale bar, 1 cm).²⁴¹ Copyright 2018, Springer Nature. B, Biodegradable semiconducting polymer ultrathin transient electronics.²⁴² Copyright 2017, National Academy of Sciences. C, Bioresorbable mechanical and temperature sensor for the brain monitoring.²⁴³ Copyright 2016, Springer Nature

Institute as the standard reference material for biocompatibility tests.²⁴⁰ In addition, Jo et al developed strain and ECG sensors with excellent permeability and biocompatibility using silk proteins.⁹² In addition to the supporting materials, the development of biocompatible active materials is also essential. For example, Choi et al reported a highly conductive and biocompatible Ag-Au NW composite for implantable electrophysiological sensors (Figure 14A).²⁴¹

Biodegradable supporting materials have been studied for years.²²⁸ Naturally derived materials (eg, cellulose, protein, and chitosan) can be decomposed under the catalysis of enzymes in the physiological environment. In addition, some synthetic polymers with degradable chemical bonds (eg, ester bonds, amide bonds, and acid anhydride bonds) as biodegradable supporting materials have been also reported.²⁴⁴ The degradation properties of synthetic polymers can be chemically controlled by adjusting the content of such chemical bonds.

Studies on degradable active substances is also very important compared to supporting materials. Combining active materials with degradable polymers is a common method, but the obtained composites are generally unstable.²⁴⁵ Therefore, Lei et al fabricated a degradable semiconducting polymer based on reversible imine bonds and building blocks, which can be decomposed within 30 days under mildly acidic conditions (Figure 14B).²⁴² Also, some inorganic active materials (eg, Mg, Zn, Fe, and Si) can be degraded under physiological conditions, which is also a

good choice for implantable physical sensors.²⁴⁶ For example, using silicon nanomembrane as raw material, Kang et al prepared a bioresorbable mechanical and temperature sensor for the brain (Figure 14C).²⁴³

6 | CONCLUSIONS AND OUTLOOK

In recent years, skin-inspired electronics have been widely studied, providing new opportunities for health monitoring, human disease diagnosis and treatment, and intelligent robots. Physical sensors are one of the key building blocks of skin-inspired electronics. In this article, we summarize the recent advances in skin-inspired mechanical sensors, temperature sensors, and humidity sensors. Meanwhile, the commonly used materials, device structures, and the practical applications of skin-inspired physical sensors are presented. In addition, several novel properties of physical sensors, such as versatility, self-healability, and implantability, are discussed.

Mechanical sensors can be divided into resistive, capacitive, piezoelectric, and triboelectric types according to working mechanisms. Among them, resistive- and capacitive-type mechanical sensors require an external power supply system, and they are more sensitive to static stimuli. In contrast, piezoelectric- and triboelectric-type mechanical sensors, which convert mechanical stimuli into voltage signals, are self-powered and are more sensitive to dynamic stimuli.

Temperature sensors can be divided into resistance temperature detectors, thermistors, and pyroelectric- and thermoelectric-type temperature sensors according to different conversion mechanisms. The resistance temperature detector is one of the most commonly used temperature sensors with higher linearity, wide working range and high stability, but with lower sensitivity. Thermistors also convert temperature stimuli into resistance changes with higher sensitivity and faster response. Pyroelectric- and thermoelectric-type temperature sensors can convert the temperature signal into a voltage signal and are self-powered temperature sensors. However, the thermoelectric-type temperature sensor requires a reference temperature during testing, which is different from other types of temperature sensors.

Humidity sensors can be divided into resistive-type sensors, capacitive-type sensors, and moisture-dependent power generators. Humidity can affect the resistivity of the active material and the capacitance of the dielectric layer. Based on this effect, researchers have developed resistive- and capacitive-type humidity sensors. In addition, humidity can generate electricity or significantly affect the voltage generated by piezoelectric or triboelectric sensors. The generated voltage can be used to detect the humidity based on the quantitative relationship between the generated voltage and humidity.

In addition, several novel properties of physical sensors, such as versatility, self-healability, and implantability have been studied. Multifunctional sensors, which can simultaneously detect various stimuli, provide new opportunities for accurately health monitoring, human disease diagnosis, and treatment. Furthermore, researchers have developed self-healing sensors that can quickly repair mechanical damage. In addition, implantable sensors, which can directly measure the physiological activities of organs and tissues, have also been developed.

However, the practical application of physical sensors for skin-inspired electronics remains challenging. Versatile sensors are required for different applying scenarios. For example, monitoring motion at joints requires large stretchability, while detecting blood pressure or sound requires high sensitivity. Therefore, it is necessary to develop physical sensors with adjustable working range. In addition, most of the reported sensors are suffered from interference from other stimuli. For example, resistive mechanical sensors have different electromechanical responses at different temperatures and humidity. Solving interference between different signals is necessary for obtaining highly sensitive and reliable physical sensors. Moreover, most physical sensors require external energy systems, which severely limits their development. Some self-powered physical sensors have low power generation and are difficult to be practically used. Therefore, the development of more efficient power supply systems or self-powered physical sensors are demanded. In

addition, although integrated multi-functional sensors composed of different physical sensors have been studied, the integration of physical sensors with chemical sensors and biosensors is still relatively rare. In addition, human-machine interaction is a new hotspot of skin-inspired electronics. Through effective human-machine interaction, people can control the robotic arms with their minds, which will expand the application field of skin-inspired electronics. More efforts should be devoted to this area in order to manifest the power of skin-inspired electronics in modern human society. In summary, with the rapid and further development of skin-inspired physical sensors, we believe that they will finally benefit the development of future health monitoring, human disease diagnosis and treatment, and intelligent robots.

ACKNOWLEDGMENTS

This work was financially supported by the National Natural Science Foundation of China (21975141, 51672153), the National Key Basic Research and Development Program (2016YFA0200103), and the National Program for Support of Top-notch Young Professionals.

CONFLICT OF INTEREST

The authors declare no conflict of interest.

ORCID

Yingying Zhang  <https://orcid.org/0000-0002-8448-3059>

REFERENCES

1. Johansson RS, Flanagan JR. Coding and use of tactile signals from the fingertips in object manipulation tasks. *Nat Rev Neurosci.* 2009;10(5):345-359.
2. Johansson RS, Birznieks I. First spikes in ensembles of human tactile afferents code complex spatial fingertip events. *Nat Neurosci.* 2004;7:170.
3. Jenmalm P, Birznieks I, Goodwin AW, Johansson RS. Influence of object shape on responses of human tactile afferents under conditions characteristic of manipulation. *Eur J Neurosci.* 2003;18(1):164-176.
4. Chortos A, Liu J, Bao Z. Pursuing prosthetic electronic skin. *Nat Mater.* 2016;15(9):937-950.
5. Huang S, Liu Y, Zhao Y, Ren Z, Guo CF. Flexible electronics: stretchable electrodes and their future. *Adv Funct Mater.* 2019;29(6):1805924.
6. Xie M, Hisano K, Zhu M, et al. Flexible multifunctional sensors for wearable and robotic applications. *Adv Mater Technol.* 2019;4(3):1800626.
7. Miyamoto A, Lee S, Cooray NF, et al. Inflammation-free, gas-permeable, lightweight, stretchable on-skin electronics with nanomeshes. *Nat Nanotechnol.* 2017;12:907.
8. Gao W, Ota H, Kiriya D, Takei K, Javey A. Flexible electronics toward wearable sensing. *Acc Chem Res.* 2019;52(3):523-533.
9. Wang X, Dong L, Zhang H, Yu R, Pan C, Wang ZL. Recent Progress in electronic skin. *Adv Sci.* 2015;2(10):1500169.

10. Trung TQ, Lee N-E. Flexible and stretchable physical sensor integrated platforms for wearable human-activity monitoring and personal healthcare. *Adv Mater.* 2016;28(22):4338-4372.
11. Tegin J, Wikander J. Tactile sensing in intelligent robotic manipulation – a review. *Ind Robot.* 2005;32(1):64-70.
12. Zang Y, Zhang F, Huang D, Gao X, Di CA, Zhu D. Flexible suspended gate organic thin-film transistors for ultra-sensitive pressure detection. *Nat Commun.* 2015;6:6269.
13. Qiao Y, Wang Y, Tian H, et al. Multilayer graphene epidermal electronic skin. *ACS Nano.* 2018;12(9):8839-8846.
14. Wang Q, Jian M, Wang C, Zhang Y. Carbonized silk nanofiber membrane for transparent and sensitive electronic skin. *Adv Funct Mater.* 2017;27(9):1605657.
15. Xia K, Wang C, Jian M, Wang Q, Zhang Y. CVD growth of fingerprint-like patterned 3D graphene film for an ultrasensitive pressure sensor. *Nano Res.* 2017;11(2):1124-1134.
16. Son D, Kang J, Vardoulis O, et al. An integrated self-healable electronic skin system fabricated via dynamic reconstruction of a nanostructured conducting network. *Nat Nanotechnol.* 2018;13(11):1057-1065.
17. Zhu Z, Li R, Pan T. Imperceptible epidermal-iontronic interface for wearable sensing. *Adv Mater.* 2018;30(6):1705122.
18. Wang X, Song WZ, You MH, et al. Bionic single-electrode electronic skin unit based on piezoelectric nanogenerator. *ACS Nano.* 2018;12(8):8588-8596.
19. Dong K, Wu Z, Deng J, et al. A stretchable yarn embedded triboelectric nanogenerator as electronic skin for biomechanical energy harvesting and multifunctional pressure sensing. *Adv Mater.* 2018;30(43):e1804944.
20. Webb RC, Bonifas AP, Behnaz A, et al. Ultrathin conformal devices for precise and continuous thermal characterization of human skin. *Nat Mater.* 2013;12:938.
21. Hong SY, Lee YH, Park H, et al. Stretchable active matrix temperature sensor array of polyaniline nanofibers for electronic skin. *Adv Mater.* 2016;28(5):930-935.
22. Zhao S, Zhu R. Electronic skin with multifunction sensors based on thermosensation. *Adv Mater.* 2017;29(15):1606151.
23. Hua Q, Sun J, Liu H, et al. Skin-inspired highly stretchable and conformable matrix networks for multifunctional sensing. *Nat Commun.* 2018;9(1):244.
24. Zhu C, Chortos A, Wang Y, et al. Stretchable temperature-sensing circuits with strain suppression based on carbon nanotube transistors. *Nat Electron.* 2018;1(3):183-190.
25. Yao S, Myers A, Malhotra A, et al. A wearable hydration sensor with conformal nanowire electrodes. *Adv Healthcare Mater.* 2017;6(6):1601159.
26. Ho DH, Sun Q, Kim SY, Han JT, Kim DH, Cho JH. Stretchable and multimodal all graphene electronic skin. *Adv Mater.* 2016;28(13):2601-2608.
27. Zhao J, Li N, Yu H, et al. Highly sensitive MoS₂ humidity sensors array for noncontact sensation. *Adv Mater.* 2017;29(34):1702076.
28. Lee S, Sasaki D, Kim D, et al. Ultrasoft electronics to monitor dynamically pulsing cardiomyocytes. *Nat Nanotechnol.* 2019;14(2):156-160.
29. Liu L, Li HY, Fan YJ, et al. Nanofiber-reinforced silver nanowires network as a robust, ultrathin, and conformable epidermal electrode for ambulatory monitoring of physiological signals. *Small.* 2019;15(22):1900755.
30. Li Y, Luo Y, Nayak S, et al. A stretchable-hybrid low-power monolithic ECG patch with microfluidic liquid-metal interconnects and stretchable carbon-black nanocomposite electrodes for wearable heart monitoring. *Adv Electron Mater.* 2019;5(2):1800463.
31. Masvidal-Codina E, Illa X, Dasilva M, et al. High-resolution mapping of infraslow cortical brain activity enabled by graphene microtransistors. *Nat Mater.* 2019;18(3):280-288.
32. Shi Z, Zheng F, Zhou Z, et al. Silk-enabled conformal multifunctional bioelectronics for investigation of spatiotemporal epileptiform activities and multimodal neural encoding/decoding. *Adv Sci.* 2019;6(9):1801617.
33. Lee JH, Hwang J-Y, Zhu J, et al. Flexible conductive composite integrated with personal earphone for wireless, real-time monitoring of electrophysiological signs. *ACS Appl Mater Interfaces.* 2018;10(25):21184-21190.
34. Li J, Song E, Chiang C-H, et al. Conductively coupled flexible silicon electronic systems for chronic neural electrophysiology. *Proc Natl Acad Sci USA.* 2018;115(41):E9542.
35. Nawrocki RA, Jin H, Lee S, Yokota T, Sekino M, Someya T. Self-adhesive and ultra-conformable, Sub-300 nm dry thin-film electrodes for surface monitoring of biopotentials. *Adv Funct Mater.* 2018;28(36):1803279.
36. Han L, Yan L, Wang M, et al. Transparent, adhesive, and conductive hydrogel for soft bioelectronics based on light-transmitting polydopamine-doped polypyrrole Nanofibrils. *Chem Mater.* 2018;30(16):5561-5572.
37. Yang S, Chen Y-C, Nicolini L, et al. "Cut-and-paste" manufacture of multiparametric epidermal sensor systems. *Adv Mater.* 2015;27(41):6423-6430.
38. Jang K-I, Jung HN, Lee JW, et al. Ferromagnetic, folded electrode composite as a soft interface to the skin for long-term electrophysiological recording. *Adv Funct Mater.* 2016;26(40):7281-7290.
39. Imani S, Bandodkar AJ, Mohan AMV, et al. A wearable chemical-electrophysiological hybrid biosensing system for real-time health and fitness monitoring. *Nat Commun.* 2016;7(1):11650.
40. Yamamoto Y, Yamamoto D, Takada M, et al. Efficient skin temperature sensor and stable gel-less sticky ECG sensor for a wearable flexible healthcare patch. *Adv Healthcare Mater.* 2017;6(17):1700495.
41. Roberts T, De Graaf JB, Nicol C, Hervé T, Flocchi M, Sanaur S. Flexible inkjet-printed multielectrode arrays for neuromuscular cartography. *Adv Healthcare Mater.* 2016;5(12):1462-1470.
42. Jeong J-W, Yeo W-H, Akhtar A, et al. Materials and optimized designs for human-machine interfaces via epidermal electronics. *Adv Mater.* 2013;25(47):6839-6846.
43. Han S, Kim MK, Wang B, Wie DS, Wang S, Lee CH. Mechanically reinforced skin-electronics with networked Nanocomposite elastomer. *Adv Mater.* 2016;28(46):10257-10265.
44. Kuzum D, Takano H, Shim E, et al. Transparent and flexible low noise graphene electrodes for simultaneous electrophysiology and neuroimaging. *Nat Commun.* 2014;5:5259.
45. Goverdovsky V, von Rosenberg W, Nakamura T, et al. Hearables: multimodal physiological in-ear sensing. *Sci Rep.* 2017;7(1):6948.
46. Debener S, Emkes R, De Vos M, Bleichner M. Unobtrusive ambulatory EEG using a smartphone and flexible printed electrodes around the ear. *Sci Rep.* 2015;5:16743.

47. Kim Y, Chortos A, Xu W, et al. A bioinspired flexible organic artificial afferent nerve. *Science*. 2018;360(6392):998-1003.
48. Lee Y, Oh JY, Kim TR, et al. Deformable organic nanowire field-effect transistors. *Adv Mater*. 2018;30(7):1704401.
49. Oh JY, Rondeau-Gagné S, Chiu Y-C, et al. Intrinsically stretchable and healable semiconducting polymer for organic transistors. *Nature*. 2016;539:411.
50. Xu J, Wang S, G-JN W, et al. Highly stretchable polymer semiconductor films through the nanoconfinement effect. *Science*. 2017;355(6320):59-64.
51. Xu J, Wu H-C, Zhu C, et al. Multi-scale ordering in highly stretchable polymer semiconducting films. *Nat Mater*. 2019;18(6):594-601.
52. Wang S, Xu J, Wang W, et al. Skin electronics from scalable fabrication of an intrinsically stretchable transistor array. *Nature*. 2018;555:83.
53. Lee Y, Oh JY, Xu W, et al. Stretchable organic optoelectronic sensorimotor synapse. *Sci Adv*. 2018;4(11):eaat7387.
54. Huang Y, Fan X, Chen S-C, Zhao N. Emerging Technologies of Flexible Pressure Sensors: materials, modeling, devices, and manufacturing. *Adv Funct Mater*. 2019;29(12):1808509.
55. Hammock ML, Chortos A, Tee BC, Tok JB, Bao Z. 25th Anniversary article: the evolution of electronic skin (e-skin): a brief history, design considerations, and recent progress. *Adv Mater*. 2013;25(42):5997-6038.
56. Abraira VE, Ginty DD. The sensory neurons of touch. *Neuron*. 2013;79(4):618-639.
57. Weber AI, Saal HP, Lieber JD, et al. Spatial and temporal codes mediate the tactile perception of natural textures. *Proc Natl Acad Sci USA*. 2013;110(42):17107-17112.
58. Scheibert J, Leurent S, Prevost A, Debrégeas G. The role of fingerprints in the coding of tactile information probed with a biomimetic sensor. *Science*. 2009;323(5920):1503-1506.
59. Craig JC, Baihua X. Temporal order and tactile patterns. *Percept Psychophys*. 1990;47(1):22-34.
60. Craig C. JMKJ. Factors affecting tactile spatial acuity. *Somatosens Mot Res*. 1998;15(1):29-45.
61. Lee MH. Tactile sensing: new directions, new challenges. *Int J Robot Res*. 2000;19(7):636-643.
62. Chou HH, Nguyen A, Chortos A, et al. A chameleon-inspired stretchable electronic skin with interactive colour changing controlled by tactile sensing. *Nat Commun*. 2015;6:8011.
63. Chen LY, Tee BCK, Chortos AL, et al. Continuous wireless pressure monitoring and mapping with ultra-small passive sensors for health monitoring and critical care. *Nat Commun*. 2014;5:5028.
64. Cookson JW. Theory of the piezo-resistive effect. *Phys Rev*. 1935;47(2):194.
65. Smith CS. Piezoresistance effect in germanium and silicon. *Phys Rev*. 1954;94(1):42.
66. Toriyama T, Sugiyama S. Analysis of piezoresistance in p-type silicon for mechanical sensors. *J Microelectromech Syst*. 2002;11(5):598-604.
67. Edwards WD, Beaulieu RP. Germanium piezoresistive element on a flexible substrate. *J Phys E Sci Instrum*. 1969;2(7):613-615.
68. Tomblor TW, Zhou C, Alexseyev L, et al. Reversible electro-mechanical characteristics of carbon nanotubes under local-probe manipulation. *Nature*. 2000;405(6788):769.
69. Bae S-H, Lee Y, Sharma BK, Lee H-J, Kim J-H, Ahn J-H. Graphene-based transparent strain sensor. *Carbon*. 2013;51:236-242.
70. Pan L, Liu G, Shi W, et al. Mechano-regulated metal-organic framework nanofilm for ultrasensitive and anti-jamming strain sensing. *Nat Commun*. 2018;9(1):3813.
71. He R, Yang P. Giant piezoresistance effect in silicon nanowires. *Nat Nanotechnol*. 2006;1(1):42-46.
72. Greil J, Lugstein A, Zeiner C, Strasser G, Bertagnolli E. Tuning the electro-optical properties of germanium nanowires by tensile strain. *Nano Lett*. 2012;12(12):6230-6234.
73. Pan L, Chortos A, Yu G, et al. An ultra-sensitive resistive pressure sensor based on hollow-sphere microstructure induced elasticity in conducting polymer film. *Nat Commun*. 2014;5:3002.
74. Yun G, Tang SY, Sun S, et al. Liquid metal-filled magnetorheological elastomer with positive piezoconductivity. *Nat Commun*. 2019;10(1):1300.
75. Timsit RS. Electrical contact resistance: properties of stationary interfaces. *IEEE Trans Compon Packag Technol*. 1999;22(1):85-98.
76. Tee BC, Wang C, Allen R, Bao Z. An electrically and mechanically self-healing composite with pressure- and flexion-sensitive properties for electronic skin applications. *Nat Nanotechnol*. 2012;7(12):825-832.
77. Fan YJ, Li X, Kuang SY, et al. Highly robust, transparent and breathable epidermal electrode. *ACS Nano*. 2018;12(9):9326-9332.
78. Muth JT, Vogt DM, Truby RL, et al. Embedded 3D printing of strain sensors within highly stretchable elastomers. *Adv Mater*. 2014;26(36):6307-6312.
79. Zhang J, Liu J, Zhuang R, Mader E, Heinrich G, Gao S. Single MWNT-glass fiber as strain sensor and switch. *Adv Mater*. 2011;23(30):3392-3397.
80. Zou B, Chen Y, Liu Y, et al. Repurposed leather with sensing capabilities for multifunctional electronic skin. *Adv Sci*. 2019;6(3):1801283.
81. He Y, Gui Q, Wang Y, Wang Z, Liao S, Wang Y. A polypyrrole elastomer based on confined polymerization in a host polymer network for highly stretchable temperature and strain sensors. *Small*. 2018;14(19):1800394.
82. You I, Choi S-E, Hwang H, Han SW, Kim JW, Jeong U. E-skin tactile sensor matrix pixelated by position-registered conductive microparticles creating pressure-sensitive selectors. *Adv Funct Mater*. 2018;28(31):1801858.
83. Yang B, Yuan W. Highly stretchable and transparent double-network hydrogel ionic conductors as flexible thermal-mechanical dual sensors and electroluminescent devices. *ACS Appl Mater Interfaces*. 2019;11(18):16765-16775.
84. Guo Y, Zhong M, Fang Z, Wan P, Yu G. A wearable transient pressure sensor made with MXene nanosheets for sensitive broad-range human-machine interfacing. *Nano Lett*. 2019;19(2):1143-1150.
85. Ma Y, Liu N, Li L, et al. A highly flexible and sensitive piezoresistive sensor based on MXene with greatly changed interlayer distances. *Nat Commun*. 2017;8(1):1207.
86. An H, Habib T, Shah S, et al. Surface-agnostic highly stretchable and bendable conductive MXene multilayers. *Sci Adv*. 2018;4(3):eaq0118.
87. Jian M, Xia K, Wang Q, et al. Flexible and highly sensitive pressure sensors based on bionic hierarchical structures. *Adv Funct Mater*. 2017;27(9):1606066.

88. Yang Z, Wang DY, Pang Y, et al. Simultaneously detecting subtle and intensive human motions based on a silver nanoparticles bridged Graphene strain sensor. *ACS Appl Mater Interfaces*. 2018;10(4):3948-3954.
89. Zhang M, Wang C, Wang H, Jian M, Hao X, Zhang Y. Carbonized cotton fabric for high-performance wearable strain sensors. *Adv Funct Mater*. 2017;27(2):1604795.
90. Chun S, Choi IY, Son W, et al. A highly sensitive force sensor with fast response based on interlocked arrays of indium tin oxide nanosprings toward human tactile perception. *Adv Funct Mater*. 2018;28(42):1804132.
91. Wang N, Xu Z, Zhan P, et al. A tunable strain sensor based on a carbon nanotubes/electrospun polyamide 6 conductive nanofibrous network embedded into poly(vinyl alcohol) with self-diagnosis capabilities. *J Mater Chem C*. 2017;5(18):4408-4418.
92. Jo M, Min K, Roy B, et al. Protein-based electronic skin akin to biological tissues. *ACS Nano*. 2018;12(6):5637-5645.
93. Wang C, Xia K, Wang H, Liang X, Yin Z, Zhang Y. Advanced carbon for flexible and wearable electronics. *Adv Mater*. 2019;31(9):1801072.
94. Wang C, Li X, Gao E, et al. Carbonized silk fabric for ultra-stretchable, highly sensitive and wearable strain sensors. *Adv Mater*. 2016;28(31):6640-6648.
95. Xu N, Hu X, Xu W, et al. Mushrooms as efficient solar steam-generation devices. *Adv Mater*. 2017;29(28):1606762.
96. Karnan M, Subramani K, Srividhya PK, Sathish M. Electrochemical studies on corn cob derived activated porous carbon for supercapacitors application in aqueous and non-aqueous electrolytes. *Electrochim Acta*. 2017;228:586-596.
97. Li Y, Samad YA, Liao K. From cotton to wearable pressure sensor. *J Mater Chem A*. 2015;3(5):2181-2187.
98. Mu J, Hou C, Wang G, et al. An elastic transparent conductor based on hierarchically wrinkled reduced graphene oxide for artificial muscles and sensors. *Adv Mater*. 2016;28(43):9491-9497.
99. Duan J, Liang X, Guo J, Zhu K, Zhang L. Ultra-stretchable and force-sensitive hydrogels reinforced with chitosan microspheres embedded in polymer networks. *Adv Mater*. 2016;28(36):8037-8044.
100. Wang Q, Ling S, Liang X, Wang H, Lu H, Zhang Y. Self-healable multifunctional electronic tattoos based on silk and graphene. *Adv Funct Mater*. 2019;29(16):1808695.
101. Ray TR, Choi J, Bandodkar AJ, et al. Bio-integrated wearable systems: a comprehensive review. *Chem Rev*. 2019;119(8):5461-5533.
102. Seyedin S, Zhang P, Naebe M, et al. Textile strain sensors: a review of the fabrication technologies, performance evaluation and applications. *Mater Horiz*. 2019;6(2):219-249.
103. Luo N, Dai W, Li C, et al. Flexible Piezoresistive sensor patch enabling ultralow power Cuffless blood pressure measurement. *Adv Funct Mater*. 2016;26(8):1178-1187.
104. Xiao X, Yuan L, Zhong J, et al. High-strain sensors based on ZnO nanowire/polystyrene hybridized flexible films. *Adv Mater*. 2011;23(45):5440-5444.
105. Yang Z, Pang Y, Han XL, et al. Graphene textile strain sensor with negative resistance variation for human motion detection. *ACS Nano*. 2018;12(9):9134-9141.
106. Zhang L, Li H, Lai X, Gao T, Yang J, Zeng X. Thiolated graphene@polyester fabric-based multilayer Piezoresistive pressure sensors for detecting human motion. *ACS Appl Mater Interfaces*. 2018;10(48):41784-41792.
107. Wang C, Xia K, Jian M, Wang H, Zhang M, Zhang Y. Carbonized silk georgette as an ultrasensitive wearable strain sensor for full-range human activity monitoring. *J Mater Chem C*. 2017;5(30):7604-7611.
108. Zhu B, Niu Z, Wang H, et al. Microstructured graphene arrays for highly sensitive flexible tactile sensors. *Small*. 2014;10(18):3625-3631.
109. Wang X, Gu Y, Xiong Z, Cui Z, Zhang T. Silk-molded flexible, ultrasensitive, and highly stable electronic skin for monitoring human physiological signals. *Adv Mater*. 2014;26(9):1336-1342.
110. Pang Y, Zhang K, Yang Z, et al. Epidermis microstructure inspired graphene pressure sensor with random distributed spinosum for high sensitivity and large linearity. *ACS Nano*. 2018;12(3):2346-2354.
111. Gao N, Zhang X, Liao S, Jia H, Wang Y. Polymer swelling induced conductive wrinkles for an ultrasensitive pressure sensor. *ACS Macro Lett*. 2016;5(7):823-827.
112. Yin F, Yang J, Peng H, Yuan W. Flexible and highly sensitive artificial electronic skin based on graphene/polyamide interlocking fabric. *J Mater Chem C*. 2018;6(25):6840-6846.
113. Yang C, Li L, Zhao J, et al. Highly sensitive wearable pressure sensors based on three-scale nested wrinkling microstructures of polypyrrole films. *ACS Appl Mater Interfaces*. 2018;10(30):25811-25818.
114. Boutry CM, Kaizawa Y, Schroeder BC, et al. A stretchable and biodegradable strain and pressure sensor for orthopaedic application. *Nat Electron*. 2018;1(5):314-321.
115. Kwon D, Lee T-I, Shim J, et al. Highly sensitive, flexible, and wearable pressure sensor based on a giant piezocapacitive effect of three-dimensional microporous elastomeric dielectric layer. *ACS Appl Mater Interfaces*. 2016;8(26):16922-16931.
116. Cho SH, Lee SW, Yu S, et al. Micropatterned pyramidal ionic gels for sensing broad-range pressures with high sensitivity. *ACS Appl Mater Interfaces*. 2017;9(11):10128-10135.
117. Yang J, Luo S, Zhou X, et al. Flexible, tunable, and ultrasensitive capacitive pressure sensor with microconformal graphene electrodes. *ACS Appl Mater Interfaces*. 2019;11(16):14997-15006.
118. Li T, Luo H, Qin L, et al. Flexible capacitive tactile sensor based on micropatterned dielectric layer. *Small*. 2016;12(36):5042-5048.
119. Kim H, Kim G, Kim T, et al. Transparent, flexible, conformal capacitive pressure sensors with nanoparticles. *Small*. 2018;14(8):1703432.
120. Lipomi DJ, Vosgueritchian M, Tee BCK, et al. Skin-like pressure and strain sensors based on transparent elastic films of carbon nanotubes. *Nat Nanotechnol*. 2011;6:788.
121. Larson C, Peele B, Li S, et al. Highly stretchable electroluminescent skin for optical signaling and tactile sensing. *Science*. 2016;351(6277):1071-1074.
122. Sun JY, Keplinger C, Whitesides GM, Suo Z. Ionic skin. *Adv Mater*. 2014;26(45):7608-7614.
123. Mannsfeld SCB, Tee BCK, Stoltenberg RM, et al. Highly sensitive flexible pressure sensors with microstructured rubber dielectric layers. *Nat Mater*. 2010;9:859.
124. Wan Y, Qiu Z, Huang J, et al. Natural plant materials as dielectric layer for highly sensitive flexible electronic skin. *Small*. 2018;14(35):e1801657.

125. Kang S, Lee J, Lee S, et al. Highly sensitive pressure sensor based on bioinspired porous structure for real-time tactile sensing. *Adv Electron Mater.* 2016;2(12):1600356.
126. Yu P, Liu W, Gu C, Cheng X, Fu X. Flexible piezoelectric tactile sensor array for dynamic three-axis force measurement. *Sensors.* 2016;16(6):819.
127. Persano L, Dagdeviren C, Su Y, et al. High performance piezoelectric devices based on aligned arrays of nanofibers of poly(vinylidene fluoride-co-trifluoroethylene). *Nat Commun.* 2013;4:1633.
128. Chen Z, Wang Z, Li X, et al. Flexible piezoelectric-induced pressure sensors for static measurements based on nanowires/graphene heterostructures. *ACS Nano.* 2017;11(5):4507-4513.
129. Hu W, Zhang C, Wang ZL. Recent progress in piezotronics and tribotronics. *Nanotechnology.* 2018;30(4):042001.
130. Tseng H-J, Tian W-C, Wu W-J. Flexible PZT thin film tactile sensor for biomedical monitoring. *Sensors.* 2013;13(5):5478-5492.
131. Wu W, Wen X, Wang ZL. Taxel-addressable matrix of vertical-nanowire piezotronic transistors for active and adaptive tactile imaging. *Science.* 2013;340(6135):952-957.
132. Kang M, Park JH, Lee KI, et al. Fully flexible and transparent piezoelectric touch sensors based on ZnO nanowires and BaTiO₃-added SiO₂ capping layers. *Phys Status Solidi A.* 2015;212(9):2005-2011.
133. Nour ES, Sandberg MO, Willander M, Nur O. Handwriting enabled harvested piezoelectric power using ZnO nanowires/polymer composite on paper substrate. *Nano Energy.* 2014;9:221-228.
134. Chorsi MT, Curry EJ, Chorsi HT, et al. Piezoelectric biomaterials for sensors and actuators. *Adv Mater.* 2019;31(1):1802084.
135. Baur C, DiMaio JR, McAllister E, et al. Enhanced piezoelectric performance from carbon fluoropolymer nanocomposites. *J Appl Phys.* 2012;112(12):124104.
136. Tao J, Bao R, Wang X, et al. Self-powered tactile sensor array systems based on the triboelectric effect. *Adv Funct Mater.* 2018;29(41):1806379.
137. Parida K, Xiong J, Zhou X, Lee PS. Progress on triboelectric nanogenerator with stretchability, self-healability and biocompatibility. *Nano Energy.* 2019;59:237-257.
138. Yi F, Zhang Z, Kang Z, Liao Q, Zhang Y. Recent advances in triboelectric nanogenerator-based health monitoring. *Adv Funct Mater.* 2019;29(41):1808849.
139. Ha M, Lim S, Cho S, et al. Skin-inspired hierarchical polymer architectures with gradient stiffness for spacer-free, ultrathin, and highly sensitive triboelectric sensors. *ACS Nano.* 2018;12(4):3964-3974.
140. Ren Z, Nie J, Shao J, et al. Fully elastic and metal-free tactile sensors for detecting both Normal and tangential forces based on triboelectric nanogenerators. *Adv Funct Mater.* 2018;28(31):1802989.
141. Zou H, Zhang Y, Guo L, et al. Quantifying the triboelectric series. *Nat Commun.* 2019;10(1):2019.
142. Fan F-R, Lin L, Zhu G, Wu W, Zhang R, Wang ZL. Transparent triboelectric nanogenerators and self-powered pressure sensors based on micropatterned plastic films. *Nano Lett.* 2012;12(6):3109-3114.
143. Wang ZL, Chen J, Lin L. Progress in triboelectric nanogenerators as a new energy technology and self-powered sensors. *Energy Environ Sci.* 2015;8(8):2250-2282.
144. Lin L, Xie Y, Wang S, et al. Triboelectric active sensor array for self-powered static and dynamic pressure detection and tactile imaging. *ACS Nano.* 2013;7(9):8266-8274.
145. Bu T, Xiao T, Yang Z, et al. Stretchable triboelectric-photonic smart skin for tactile and gesture sensing. *Adv Mater.* 2018;30(16):1800066.
146. Jiang X-Z, Sun Y-J, Fan Z, Zhang T-Y. Integrated flexible, waterproof, transparent, and self-powered tactile sensing panel. *ACS Nano.* 2016;10(8):7696-7704.
147. Pu X, Liu M, Chen X, et al. Ultrastretchable, transparent triboelectric nanogenerator as electronic skin for biomechanical energy harvesting and tactile sensing. *Sci Adv.* 2017;3(5):e1700015.
148. Guo H, Li T, Cao X, et al. Self-sterilized flexible single-electrode triboelectric nanogenerator for energy harvesting and dynamic force sensing. *ACS Nano.* 2017;11(1):856-864.
149. Wang S, Lin L, Wang ZL. Triboelectric nanogenerators as self-powered active sensors. *Nano Energy.* 2015;11:436-462.
150. Ramuz M, Tee BC-K, Tok JB-H, Bao Z. Transparent, optical, pressure-sensitive artificial skin for large-area stretchable electronics. *Adv Mater.* 2012;24(24):3223-3227.
151. Dykes RW. Coding of steady and transient temperatures by cutaneous "cold" fibers serving the hand of monkeys. *Brain Res.* 1975;98(3):485-500.
152. Youn D-Y, Jung U, Naqi M, et al. Wireless real-time temperature monitoring of blood packages: silver nanowire-embedded flexible temperature sensors. *ACS Appl Mater Interfaces.* 2018;10(51):44678-44685.
153. Harada S, Kanao K, Yamamoto Y, Arie T, Akita S, Takei K. Fully printed flexible fingerprint-like three-axis tactile and slip force and temperature sensors for artificial skin. *ACS Nano.* 2014;8(12):12851-12857.
154. Tien NT, Jeon S, Kim D-I, et al. A flexible bimodal sensor array for simultaneous sensing of pressure and temperature. *Adv Mater.* 2014;26(5):796-804.
155. Jung M, Kim K, Kim B, et al. Paper-based bimodal sensor for electronic skin applications. *ACS Appl Mater Interfaces.* 2017;9(32):26974-26982.
156. Imran M, Bhattacharyya A. Effect of thin film thicknesses and materials on the response of RTDs and microthermocouples. *IEEE Sens J.* 2006;6(6):1459-1467.
157. Kim D-H, Lu N, Ma R, et al. Epidermal Electronics. *Science.* 2011;333(6044):838-843.
158. Salvatore GA, Sülzle J, Dalla Valle F, et al. Biodegradable and highly deformable temperature sensors for the internet of things. *Adv Funct Mater.* 2017;27(35):1702390.
159. Xu L, Gutbrod SR, Bonifas AP, et al. 3D multifunctional integumentary membranes for spatiotemporal cardiac measurements and stimulation across the entire epicardium. *Nat Commun.* 2014;5:3329.
160. Yan C, Wang J, Lee PS. Stretchable graphene thermistor with tunable thermal index. *ACS Nano.* 2015;9(2):2130-2137.
161. Zhao J, Zhang Y, Huang Y, et al. 3D printing fiber electrodes for an all-fiber integrated electronic device via hybridization of an asymmetric supercapacitor and a temperature sensor. *Adv Sci.* 2018;5(11):1801114.
162. Yokota T, Inoue Y, Terakawa Y, et al. Ultraflexible, large-area, physiological temperature sensors for multipoint measurements. *Proc Natl Acad Sci USA.* 2015;112(47):14533-14538.

163. Oh JH, Hong SY, Park H, et al. Fabrication of high-sensitivity skin-attachable temperature sensors with bioinspired microstructured adhesive. *ACS Appl Mater Interfaces*. 2018;10(8):7263-7270.
164. Feteira A. Negative temperature coefficient resistance (NTCR) ceramic thermistors: An industrial perspective. *J Am Ceram Soc*. 2009;92(5):967-983.
165. Katerinopoulou D, Zalar P, Sweelssen J, et al. Large-area all-printed temperature sensing surfaces using novel composite thermistor materials. *Adv Electron Mater*. 2019;5(2):1800605.
166. Sun B, McCay RN, Goswami S, et al. Gas-permeable, multifunctional on-skin electronics based on laser-induced porous graphene and sugar-templated elastomer sponges. *Adv Mater*. 2018;30(50):1804327.
167. Vuorinen T, Niittynen J, Kankkunen T, Kraft TM, Mäntysalo M. Inkjet-printed graphene/PEDOT:PSS temperature sensors on a skin-conformable polyurethane substrate. *Sci Rep*. 2016;6:35289.
168. Zeng Y, Lu G, Wang H, Du J, Ying Z, Liu C. Positive temperature coefficient thermistors based on carbon nanotube/polymer composites. *Sci Rep*. 2014;4:6684.
169. Jeon J, Lee H-B-R, Bao Z. Flexible wireless temperature sensors based on Ni microparticle-filled binary polymer composites. *Adv Mater*. 2013;25(6):850-855.
170. Trung TQ, Ramasundaram S, Hwang B-U, Lee N-E. An all-elastomeric transparent and stretchable temperature sensor for body-attachable wearable electronics. *Adv Mater*. 2016;28(3):502-509.
171. Trung TQ, Dang TML, Ramasundaram S, Toi PT, Park SY, Lee N-E. A stretchable strain-insensitive temperature sensor based on free-standing elastomeric composite fibers for on-body monitoring of skin temperature. *ACS Appl Mater Interfaces*. 2019;11(2):2317-2327.
172. Xue H, Yang Q, Wang D, et al. A wearable pyroelectric nanogenerator and self-powered breathing sensor. *Nano Energy*. 2017;38:147-154.
173. Chen Y, Zhang Y, Yuan F, Ding F, Schmidt OG. A flexible PMN-PT ribbon-based piezoelectric-pyroelectric hybrid generator for human-activity energy harvesting and monitoring. *Adv Electron Mater*. 2017;3(3):1600540.
174. Zhang F, Zang Y, Huang D, Di C-a, Zhu D. Flexible and self-powered temperature-pressure dual-parameter sensors using microstructure-frame-supported organic thermoelectric materials. *Nat Commun*. 2015;6:8356.
175. Sebald G, Guyomar D, Agbossou A. On thermoelectric and pyroelectric energy harvesting. *Smart Mater Struct*. 2009;18(12):125006.
176. Bowen CR, Taylor J, LeBoulbar E, Zabek D, Chauhan A, Vaish R. Pyroelectric materials and devices for energy harvesting applications. *Energy Environ Sci*. 2014;7(12):3836-3856.
177. Izyumskaya N, Alivov Y, Cho SJ, Morkoc H, Lee H, Kang YS. Processing, structure, properties, and applications of PZT thin films. *Crit Rev Solid State Mater Sci*. 2007;32(3-4):111-202.
178. Kong LB, Zhang TS, Ma J, Boey F. Progress in synthesis of ferroelectric ceramic materials via high-energy mechanochemical technique. *Prog Mater Sci*. 2008;53(2):207-322.
179. Qiu XL. Patterned piezo-, pyro-, and ferroelectricity of poled polymer electrets. *J Appl Phys*. 2010;108(1):19.
180. Wan C, Bowen CR. Multiscale-structuring of polyvinylidene fluoride for energy harvesting: the impact of molecular-, micro- and macro-structure. *J Mater Chem A*. 2017;5(7):3091-3128.
181. Viola FA, Spanu A, Ricci PC, Bonfiglio A, Cosseddu P. Ultrathin, flexible and multimodal tactile sensors based on organic field-effect transistors. *Sci Rep*. 2018;8(1):8073.
182. Yang Y, Zhang H, Zhu G, Lee S, Lin Z-H, Wang ZL. Flexible hybrid energy cell for simultaneously harvesting thermal, mechanical, and solar energies. *ACS Nano*. 2013;7(1):785-790.
183. Tien NT, Seol YG, Dao LHA, Noh HY, Lee N-E. Utilizing highly crystalline pyroelectric material as functional gate dielectric in organic thin-film transistors. *Adv Mater*. 2009;21(8):910-915.
184. Lee JS, Shin K-Y, Cheong OJ, Kim JH, Jang J. Highly sensitive and multifunctional tactile sensor using free-standing ZnO/-PVDF thin film with graphene electrodes for pressure and temperature monitoring. *Sci Rep*. 2015;5:7887.
185. Park J, Kim M, Lee Y, Lee HS, Ko H. Fingertip skin-inspired microstructured ferroelectric skins discriminate static/dynamic pressure and temperature stimuli. *Sci Adv*. 2015;1(9):e1500661.
186. Van Herwaarden A, Sarro P. Thermal sensors based on the Seebeck effect. *Sens Actuat*. 1986;10(3-4):321-346.
187. Chen R, Lee J, Lee W, Li D. Thermoelectrics of nanowires. *Chem Rev*. 2019;119(15):9260-9302.
188. Majumdar A. Thermoelectricity in semiconductor nanostructures. *Science*. 2004;303(5659):777.
189. Kasap S. *Thermoelectric Effects in Metals: Thermocouples*. Saskatoon, Canada: Department of Electrical Engineering University of Saskatchewan; 2001.
190. Wang H, Ail U, Gabriellson R, Berggren M, Crispin X. Ionic Seebeck effect in conducting polymers. *Adv Energy Mater*. 2015;5(11):1500044.
191. Han S, Alvi NUH, Granlöv L, et al. A multiparameter pressure-temperature-humidity sensor based on mixed ionic-electronic cellulose aerogels. *Adv Sci*. 2019;6(8):1802128.
192. Petsagkourakis I, Kim N, Tybrandt K, Zozoulenko I, Crispin X. Poly(3,4-ethylenedioxythiophene): chemical synthesis, transport properties, and thermoelectric devices. *Adv Electron Mater*. 2019;5(11):1800918.
193. Dragoman D, Dragoman M. Giant thermoelectric effect in graphene. *Appl Phys Lett*. 2007;91(20):203116.
194. Hong SY, Oh JH, Park H, et al. Polyurethane foam coated with a multi-walled carbon nanotube/polyaniline nanocomposite for a skin-like stretchable array of multi-functional sensors. *NPG Asia Mater*. 2017;9:e448.
195. Park KT, Choi J, Lee B, et al. High-performance thermoelectric bracelet based on carbon nanotube ink printed directly onto a flexible cable. *J Mater Chem A*. 2018;6(40):19727-19734.
196. Hou C, Wang H, Zhang Q, Li Y, Zhu M. Highly conductive, flexible, and compressible all-graphene passive electronic skin for sensing human touch. *Adv Mater*. 2014;26(29):5018-5024.
197. Tung TT, Pham-Huu C, Janowska I, Kim T, Castro M, Feller J-F. Hybrid films of graphene and carbon nanotubes for high performance chemical and temperature sensing applications. *Small*. 2015;11(28):3485-3493.
198. Taroni PJ, Santagiuliana G, Wan K, et al. Toward stretchable self-powered sensors based on the thermoelectric response of PEDOT: PSS/polyurethane blends. *Adv Funct Mater*. 2018;28(15):1704285.
199. Ota H, Chen K, Lin Y, et al. Highly deformable liquid-state heterojunction sensors. *Nat Commun*. 2014;5:5032.
200. Zou Z, Zhu C, Li Y, Lei X, Zhang W, Xiao J. Rehealable, fully recyclable, and malleable electronic skin enabled by

- dynamic covalent thermoset nanocomposite. *Sci Adv.* 2018; 4(2):eaq0508.
201. Ackerley R, Olausson H, Wessberg J, McGlone F. Wetness perception across body sites. *Neurosci Lett.* 2012;522(1):73-77.
 202. Chen Z, Lu C. Humidity sensors: a review of materials and mechanisms. *Sens Lett.* 2005;3(4):274-295.
 203. Huang X, Cheng H, Chen K, et al. Epidermal impedance sensing sheets for precision hydration assessment and spatial mapping. *IEEE Trans Biomed Eng.* 2013;60(10):2848-2857.
 204. Guo H, Chen J, Tian L, Leng Q, Xi Y, Hu C. Airflow-induced triboelectric nanogenerator as a self-powered sensor for detecting humidity and airflow rate. *ACS Appl Mater Interfaces.* 2014;6(19):17184-17189.
 205. Hu K, Xiong R, Guo H, et al. Self-powered electronic skin with biotactile selectivity. *Adv Mater.* 2016;28(18):3549-3556.
 206. He H, Fu Y, Zang W, et al. A flexible self-powered T-ZnO/PVDF/fabric electronic-skin with multi-functions of tactile-perception, atmosphere-detection and self-clean. *Nano Energy.* 2017;31:37-48.
 207. Shen D, Xiao M, Xiao Y, et al. Self-powered, rapid-response, and highly flexible humidity sensors based on moisture-dependent voltage generation. *ACS Appl Mater Interfaces.* 2019;11(15):14249-14255.
 208. Shen D, Xiao M, Zou G, Liu L, Duley WW, Zhou YN. Self-powered wearable electronics based on moisture enabled electricity generation. *Adv Mater.* 2018;30(18):1705925.
 209. Yang C, Huang Y, Cheng H, Jiang L, Qu L. Rollable, stretchable, and reconfigurable graphene hygroelectric generators. *Adv Mater.* 2019;31(2):1805705.
 210. Wu J, Sun Y-M, Wu Z, et al. Carbon nanocoil-based fast-response and flexible humidity sensor for multifunctional applications. *ACS Appl Mater Interfaces.* 2019;11(4):4242-4251.
 211. Zhao X, Long Y, Yang T, Li J, Zhu H. Simultaneous high sensitivity sensing of temperature and humidity with graphene woven fabrics. *ACS Appl Mater Interfaces.* 2017;9(35):30171-30176.
 212. Wang X, Xiong Z, Liu Z, Zhang T. Exfoliation at the liquid/air interface to assemble reduced graphene oxide ultrathin films for a flexible noncontact sensing device. *Adv Mater.* 2015;27(8):1370-1375.
 213. Ye M, Zhang Z, Zhao Y, Qu L. Graphene platforms for smart energy generation and storage. *Joule.* 2018;2(2):245-268.
 214. Zhao F, Cheng H, Zhang Z, Jiang L, Qu L. Direct power generation from a graphene oxide film under moisture. *Adv Mater.* 2015;27(29):4351-4357.
 215. Huang Y, Cheng H, Yang C, et al. Interface-mediated hygroelectric generator with an output voltage approaching 1.5 volts. *Nat Commun.* 2018;9(1):4166.
 216. Huang Y, Cheng H, Yang C, Yao H, Li C, Qu L. All-region-applicable, continuous power supply of graphene oxide composite. *Energy Environ Sci.* 2019;12(6):1848-1856.
 217. Liang Y, Zhao F, Cheng Z, et al. Self-powered wearable graphene fiber for information expression. *Nano Energy.* 2017; 32:329-335.
 218. Liang Y, Zhao F, Cheng Z, et al. Electric power generation via asymmetric moisturizing of graphene oxide for flexible, printable and portable electronics. *Energy Environ Sci.* 2018;11(7):1730-1735.
 219. Sreepasad TS, Rodriguez AA, Colston J, et al. Electron-tunneling modulation in percolating network of graphene quantum dots: fabrication, phenomenological understanding, and humidity/pressure sensing applications. *Nano Lett.* 2013;13(4):1757-1763.
 220. Kim SY, Park S, Park HW, Park DH, Jeong Y, Kim DH. Highly sensitive and multimodal all-carbon skin sensors capable of simultaneously detecting tactile and biological stimuli. *Adv Mater.* 2015;27(28):4178-4185.
 221. Zhao F, Zhao Y, Cheng H, Qu L. A graphene fibriform resporator for sensing heat, humidity, and mechanical changes. *Angew Chem Int Ed.* 2015;54(49):14951-14955.
 222. Li T, Li L, Sun H, et al. Porous ionic membrane based flexible humidity sensor and its multifunctional applications. *Adv Sci.* 2017;4(5):1600404.
 223. Park YD, Kang B, Lim HS, Cho K, Kang MS, Cho JH. Polyelectrolyte interlayer for ultra-sensitive organic transistor humidity sensors. *ACS Appl Mater Interfaces.* 2013;5(17):8591-8596.
 224. Dai J, Zhao H, Lin X, et al. Ultrafast response polyelectrolyte humidity sensor for respiration monitoring. *ACS Appl Mater Interfaces.* 2019;11(6):6483-6490.
 225. Guo H, Lan C, Zhou Z, Sun P, Wei D, Li C. Transparent, flexible, and stretchable WS₂ based humidity sensors for electronic skin. *Nanoscale.* 2017;9(19):6246-6253.
 226. Bae GY, Han JT, Lee G, et al. Pressure/temperature sensing bimodal electronic skin with stimulus discriminability and linear sensitivity. *Adv Mater.* 2018;30(43):e1803388.
 227. Kang J, Tok JBH, Bao Z. Self-healing soft electronics. *Nat Electron.* 2019;2(4):144-150.
 228. Yu X, Shou W, Mahajan BK, Huang X, Pan H. Materials, processes, and facile manufacturing for bioresorbable electronics: a review. *Adv Mater.* 2018;30(28):1707624.
 229. Steiger C, Abramson A, Nadeau P, Chandrakasan AP, Langer R, Traverso G. Ingestible electronics for diagnostics and therapy. *Nat Rev Mater.* 2019;4(2):83-98.
 230. Wang C, Xia K, Zhang M, Jian M, Zhang Y. An all-silk-derived dual-mode E-skin for simultaneous temperature-pressure detection. *ACS Appl Mater Interfaces.* 2017;9(45):39484-39492.
 231. Zhang M, Sun JJ, Khatib M, et al. Time-space-resolved origami hierarchical electronics for ultrasensitive detection of physical and chemical stimuli. *Nat Commun.* 2019;10(1):2019.
 232. Nakata S, Shiomi M, Fujita Y, Arie T, Akita S, Takei K. A wearable pH sensor with high sensitivity based on a flexible charge-coupled device. *Nature Electron.* 2018;1(11):596-603.
 233. Wang S, Oh JY, Xu J, Tran H, Bao Z. Skin-inspired electronics: An emerging paradigm. *Acc Chem Res.* 2018;51(5):1033-1045.
 234. White SR, Sottos NR, Geubelle PH, et al. Autonomic healing of polymer composites. *Nature.* 2001;409(6822):794-797.
 235. Kang J, Son D, Wang GN, et al. Tough and water-insensitive self-healing elastomer for robust electronic skin. *Adv Mater.* 2018;30(13):e1706846.
 236. Cao Y, Tan YJ, Li S, et al. Self-healing electronic skins for aquatic environments. *Nat Electron.* 2019;2(2):75-82.
 237. Wang C, Liu N, Allen R, et al. A rapid and efficient self-healing thermo-reversible elastomer crosslinked with graphene oxide. *Adv Mater.* 2013;25(40):5785-5790.
 238. He Y, Liao S, Jia H, Cao Y, Wang Z, Wang Y. A self-healing electronic sensor based on thermal-sensitive fluids. *Adv Mater.* 2015;27(31):4622-4627.
 239. Irimia-Vladu M. "Green" electronics: biodegradable and biocompatible materials and devices for sustainable future. *Chem Soc Rev.* 2014;43(2):588-610.
 240. Bélanger MC, Marois Y. Hemocompatibility, biocompatibility, inflammatory and in vivo studies of primary reference

materials low-density polyethylene and polydimethylsiloxane: a review. *J Biomed Mater Res*. 2001;58(5):467-477.

241. Choi S, Han SI, Jung D, et al. Highly conductive, stretchable and biocompatible Ag-Au core-sheath nanowire composite for wearable and implantable bioelectronics. *Nat Nanotechnol*. 2018;13(11):1048-1056.
242. Lei T, Guan M, Liu J, et al. Biocompatible and totally disintegrable semiconducting polymer for ultrathin and ultralightweight transient electronics. *Proc Natl Acad Sci USA*. 2017;114(20):01478.
243. Kang S-K, Murphy RKJ, Hwang S-W, et al. Bioresorbable silicon electronic sensors for the brain. *Nature*. 2016;530:71.
244. Serrano MC, Chung EJ, Ameer GA. Advances and applications of biodegradable elastomers in regenerative medicine. *Adv Funct Mater*. 2010;20(2):192-208.
245. Dvir T, Timko BP, Brigham MD, et al. Nanowired three-dimensional cardiac patches. *Nat Nanotechnol*. 2011;6:720.
246. Boutry CM, Nguyen A, Lawal QO, Chortos A, Rondeau-Gagné S, Bao Z. A sensitive and biodegradable pressure sensor array for cardiovascular monitoring. *Adv Mater*. 2015;27(43):6954-6961.
247. Kim K, Jung M, Kim B, et al. Low-voltage, high-sensitivity and high-reliability bimodal sensor array with fully inkjet-printed flexible conducting electrode for low power consumption electronic skin. *Nano Energy*. 2017;41:301-307.
248. Kim GH, Shao L, Zhang K, Pipe KP. Engineered doping of organic semiconductors for enhanced thermoelectric efficiency. *Nat Mater*. 2013;12:719.
249. Tan YJ, Wu J, Li H, Tee BCK. Self-healing electronic materials for a smart and sustainable future. *ACS Appl Mater Interfaces*. 2018;10(18):15331-15345.
250. Teng L, Ye S, Handschuh-Wang S, Zhou X, Gan T, Zhou X. Liquid metal-based transient circuits for flexible and recyclable electronics. *Adv Funct Mater*. 2019;29(11):1808739.

AUTHOR BIOGRAPHIES



Shuo Li received his BS degree in material chemistry from Central South University in 2018. He is currently a PhD candidate at the Department of Chemistry, Tsinghua University, China. His current research interest is silk fibroin/carbon-based materials and their applications in skin-inspired electronics.

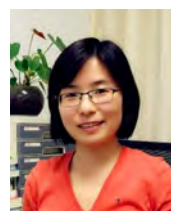


Yong Zhang received his PhD degree in physical chemistry from Shandong University in 2019. He is currently a postdoctoral fellowship in Prof. Zhang's Group at the Department of Chemistry, Tsinghua University, China. His current research

interest is the development of advanced fiber materials for E-textiles.



Yiliang Wang received his PhD degree in materials science and engineering from Beijing Institute of Technology in 2017. He is currently a postdoctoral fellowship in Prof. Zhang's Group at the Department of Chemistry, Tsinghua University, China. His research interests include polymer modification, carbon materials, hydrogels, 3D printing and their applications in flexible electronics.



Yingying Zhang received her PhD degree in physical chemistry from Peking University in 2007. From June 2008 to June 2011, she worked in Los Alamos National Laboratory (USA) as a postdoctoral research associate. Then, she joined Tsinghua University as an associate professor in July of 2011. Her research focuses on the design and controlled preparation of nanocarbon, silk, and their hybrid materials, aiming to develop high performance flexible electronics and wearable systems. She has authored more than 90 journal papers with over 3000 citations. Besides, she has authored 1 book and 2 book chapters, and 12 awarded patents. She has been supported/awarded by National Science Fund for Excellent Young Scholar (2014), National Program for Support of Top-notch Young Professionals (2016), and Young Scholars of Yangtze River scholar professor program (2017).

How to cite this article: Li S, Zhang Y, Wang Y, et al. Physical sensors for skin-inspired electronics. *InfoMat*. 2019;1-28. <https://doi.org/10.1002/inf2.12060>